Automation of membrane based solvent extraction for Zr and Hf separation

K Meerholz
20770669
B.Sc. Industrial Science

Dissertation submitted in partial fulfillment of the requirements for the degree *Magister Scientiae* in Chemistry at the Potchefstroom Campus of the North-West University

Supervisor: Mr DJ van der Westhuizen
Co-supervisor: Prof HM Krieg

November 2015

ACKNOWLEDGEMENTS

The author would like to thank the following people and organisations for their contribution to the completion of this study:

- Mr Derik van der Westhuizen for his leadership, help and supervision to help me complete this study.

- Prof Henning Krieg for his contribution and supervision, in particular to his help with the writing of this document.

- Financial support supplied by the Advance Metals Initiative (AMI), which is a Department of Technology (DST) of South Africa initiative.

- Dr Johan Nel and the Nuclear Metals Development Network (NMDN), which is a division of AMI that is managed by the South African Nuclear Energy Corporation (Necsa), for the opportunity to be part of this research group.

- The North-West University (NWU) and the Chemical Resource Beneficiation (CRB) for the financial support and use of the academic institutions equipment and expertise.

- Dr Andries Kruger for his insight into the process design and help with the automation and control program.

- Ms Hestelle Stoppel for all the help with the financial administration.

- To my colleagues and friends for their friendship and help during this study.

- To my family for their continued moral and financial support.

ABSTRACT

In recent years, research into metal ion extraction using hollow fibre membranes has grown, focussing on the extraction of a wide range of metals including base, transition, and rare earth metals. This nondispersive solvent extraction technique does not have many of the disadvantages such as emulsion formation, foaming, and flooding, which are associated with the more traditional dispersive solvent extraction techniques. Current studies using hollow fibre membranes for the separation of Zr and Hf generally use the same experimental setup consisting of a manually controlled system monitored by analogue gauges. Although the manual system is sufficient for initial proof of concept studies, it does lack the accuracy and repeatability to advance this technology to the next step of commercialisation. The aim of this study was therefore to design, simulate and construct an automated membrane based solvent extraction (AMBSX) system for use in Zr and Hf extraction research. Boundary conditions entailed that the system should be chemically resistant to acids (up to 9 mol/L) as well as to a variety of organic solvents commonly used in solvent extraction. In addition, the apparatus was designed to be able to function over a range of pressures (0-200 kPa), flow rates (100 - 900 mL/min) and flow directions (co- and counter-current) up to a temperature of 35 °C. The objective was to attain independent automated control of both flow rate and pressure in the system, while improving the accuracy and repeatability of the results.

The automation of the experimental setup was done using National Instruments hardware and a central controller programmed using LabVIEW™. The system was first simulated using LabVIEW's built in simulation functionality as a proof of concept for the control of the system. Flow rate and pressure were controlled using proportional derivative and integral (PID) control algorithms and optimised using the Cohen-Coon tuning method. It was shown that proportional integral (PI) control was preferential for the AMBSX system. After the design, construction and commissioning of the AMBSX, the system was optimised using the method obtained from the simulation of the AMBSX. After optimisation, a case study for the extraction of Zr and Hf, using Cyanex 301® as extractant, was conducted on the AMBSX using pressures of 100 kPa and 70 kPa and flow rates of 450 mL/min and 350 mL/min for the aqueous and organic phases, respectively. Five separate runs of 120 minutes each were done to determine the control and repeatability obtainable with the AMBSX. It was shown that the automated system was able to accurately control the flow rate and pressure to desired set points. This improvement of accuracy led to highly reproducible extraction results with the standard deviations between the five extractions varying by less than 1.2%. From this it can be concluded that the design, simulation and construction of an automated system was successfully implemented with independent control of the flow rate and pressure.

Key Words: Membrane based solvent extraction; automation; LabVIEW™; Zirconium; Hafnium

TABLE OF CONTENTS

LIST OF FIGURES

LIST OF TABLES

NOMENCLATURE

AMBSX	Automated membrane based solvent extraction
Cyanex 301®	bis(2,4,4-trimethylpentyl)dithiophosphinic acid
DCS	distributed control systems
FPGA	Field-programmable gate array
GUI	Graphical user interface
I/O	Input/output
ICP-OES	Inductively coupled plasma optical emission spectrometer
mA	milliampere
MBSX	Membrane based solvent extraction
NI	National Instruments
PFA	perfluoroalkoxy alkanes
PFD	Process flow diagram
PID	Proportional integral derivative control algorithm
PLC	programmable logic controller
PP	Polypropylene
PTFE	polytetrafluoroethylene
PVDF	polyvinylidene fluoride
RTD	Resistance temperature detectors
SX	Solvent extraction
UI	User interface
V DC	Volt direct current

CHAPTER 1: INTRODUCTION

1.1. Introduction

As the energy consumption of the world increases, more sustainable forms of power generation become increasingly important. Nuclear power is an example of a sustainable form of energy; however, the production of nuclear waste is of concern. The low, medium and high level nuclear waste that is generated must be isolated from the biosphere indefinitely [1]. While the spent fuel is the most important contributor to the waste, an improvement of the materials used in nuclear reactors will help reduce the production of waste by increasing the reactor's service life. Crucial to the reactor is the fuel housings that contain the enriched uranium. This cladding is currently made from zirconium (Zr) alloys. Zr alloys as cladding for fuel rods have been an essential element of the nuclear energy industry for the past five decades [2]. The choice of Zr is based on its chemical and physical properties, which make it ideal for use in the reactor cores.

Zr is a hard and ductile transition metal and is silver in appearance. The most important source of Zr in nature is Zircon ore, which is a silicate oxide that can be found in coastal and river sand deposits, with the largest zircon mines found in India, Sri Lanka, Australia and South Africa. Zircon is also a main source of the metal hafnium (Hf), which makes up 2-5%wt of zircon sources [3]. Zr was first discovered in 1789, but was only named in 1797. The first purified Zr metal was produced in 1925, coinciding with the development of nuclear science, by reducing vaporised Zr tetraiodide (ZrI_4) on a heated tungsten filament.

Hf is commonly found in naturally occurring Zr sources. Hf is a heavy transition metal, falling in Group 4 of the periodic table with Zr and titanium (Ti). It is white-grey in appearance and is less malleable than Zr. Hf was only discovered as late as 1923, 134 years after the discovery of Zr. This was due to the similarity between the two metals, which made it difficult to differentiate the one from the other. Hf is mainly produced as the by-product of the Zr purification process. Its current industrial applications are as strengthening agent in nickel alloys, and as temperature control rods used in nuclear reactors.

Zr's high melting point of 2125 K, high corrosion resistance, low hydrogen absorption, and most significantly its low thermal neutron absorption cross section of 0.2×10^{-28} m^2/atom make it an ideal candidate as cladding material for nuclear Light Water Reactors [4-6], as the cross section of Zr allows neutrons to pass through the fuel cladding without being absorbed. However, the 1-3%wt Hf contained in zircon ores has a high thermal neutron absorption cross section, which is approximately 600 times larger than that of Zr. When retained in the Zr, this contamination increases the neutron absorption, thereby diminishing the performance of the alloy. It is thus important that the Hf is separated from the Zr to increase the service life of the components made from Zr alloys. The production of nuclear grade Zr that has less than 100 ppm Hf contamination is an intricate and costly process as Zr and Hf have similar physical and chemical properties [7].

Currently industrial processes that produce nuclear grade Zr [8] have inherent problems, the most important of which entails the inefficiency and cost of the production of such purified metals.

The purification of Zr to a nuclear grade has large economic potential for South Africa; however, currently the zircon is refined to zirconia and exported without further beneficiation. Thus an initiative was started by the Department of Science and Technology (DST), South Africa that launched the Advanced Metals Initiative (AMI). The South African Nuclear Energy Corporation SOC Limited (Necsa), due to existing expertise and infrastructure, was entrusted to investigate the manufacturing of nuclear metals, thereby establishing the Nuclear Metals Development Network (NMDN) Hub of the AMI. Solvent extraction (SX) was identified as a potential technique for this separation [9-15]. SX involves the selective separation of the dissolved metal species into two immiscible liquids, namely an acidic aqueous medium that contains the dissolved metal salts and an organic solvent that contains an extractant [8]. While SX is considered a viable means in the hydrometallurgical method of metal ion extraction, the technique is a batch to semi-batch method, which has disadvantages when scaling to an industrial size setup [13]. Subsequently, a method for continuous flow was developed for SX using mixer-settlers; however, mixer settlers require large areas to allow phase separation to occur. The combination with large volumes of flammable organic solvents can prove dangerous when large volumes of low ignition point fumes are produced [16]. In addition to scaling problems, SX has a detrimental problem of 3rd phase formation (or emulsion formation), which can sometimes be avoided by adding phase modifiers to the organic phase.

A solution to 3rd phase formation was attained by the introduction of hollow fibre membrane contactors. The contactors allow the mass transfer to occur without the mixing of phases. During membrane based solvent extraction (MBSX) the organic phase is, for example, immobilised in the pores of a hollow fibre membrane, while the aqueous phase is forced onto the surface of the fibres using a pressure differential. This creates contacting surfaces at micro sites at the membrane pores, allowing mass transfer to take place without a mixing of the phases [17]. This approach allows a more continuous process, enabling methods such as a cascade process to be used [18,19]. Due to its advantages, MBSX has been used in a variety of metal separations including zinc, vanadium, molybdenum, mercury, neodymium and platinum group metals [20-24]. In 2012, an MBSX technique for separation of Zr and Hf was patented [25].

Apart from the avoidance of 3rd phase formation, MBSX has additional advantages including ease to scale up to industrial size due to the absence of moving parts within the membrane. Since membranes have a modular design, additional modules can simply be added if more contact area is needed. Furthermore, MBSX has a low loss and retention of solvents which is important when expensive solvents are used. The MBSX allows for a larger range of flow rates and flow directions as compared to other liquid-liquid extraction techniques. In addition, MBSX allows for the

concentration of streams by using ratios that are less than 1:1. Since the membrane contact area is known, it is easy to predict and optimise extraction performance [26]. Although this method has been extensively used for laboratory scale investigations, the experimental setup always remained manually operated [27-31].

1.2. Problem statement

With an increased use of hollow fibre membranes in hydrometallurgical processes [13,26], the need for an accurate, controlled experimental setup has arisen. The manually operated MBSX setup used to date has many fundamental design flaws, including: i) the repeatability and accuracy studies proved to be problematic, ii) high chemical consumption due to large internal volumes, iii) turbulent flow through the system caused erratic pressure spikes, iv) lack of control lead to flow rate and pressure drifts over extended contact times, occasionally leading to breakthrough of the organic phase into the aqueous phase, v) flow rates had to be manually calibrated and operated before each experiment with no independent pressure and flow control, and vi) experimental parameters and data had to be recorded manually.

1.3. Aim and objectives

The aim of this study is to design, program and build an automated hollow fibre membrane based solvent extraction (AMBSX) unit that is capable of increased control and monitoring of MBSX research, thereby providing more repeatable and consistent data of the MBSX process. The disadvantages of the MBSX will be addressed by automating the system. The automisation will be attained by first designing, simulating and then constructing an AMBSX for the use in studies of metal ion extraction, specifically but not limited to the Zr/Hf separation that has been optimised using batch SX. The AMBSX will have a level of automisation to reduce human input, but it will also have to include digital metering equipment for the capture of data during an experiment. The system must enable flow rate and pressure control to be independent from one another, enabling a larger range of experiments into the mass transfer and kinetics of the AMBSX process.

The AMBSX must be able to control and measure flow rate and pressure of both aqueous and organic streams, where control will be achieved with proportional integral derivative (PID) control by first simulating the system before applying it to the AMBSX. The flow rate must be variable from 100 ml/min to 1000 ml/min. The internal pressure across the membrane must be controllable and have a maximum pressure of 200 kPa. The AMBSX must be chemically compatible with hydrochloric acid (HCl), nitric acid (HNO_3) and sulphuric acid (H_2SO_4) up to a concentration of 9 mol/L for the aqueous stream, while the organic stream must be able to handle organic acids and

hydrocarbon solvents. This will ensure that the AMBSX is compatible with a large variety of experiments. The AMBSX must have a cleaning procedure built into the system and also be able to change flow direction across the membrane to enable either counter-current or co-current experiments. To attain this, the following objectives were set:

- A literature survey will be completed on current Zr/Hf SX and MBSX separation techniques, including MBSX kinetic and optimization studies.
- A system will be designed and a detailed process flow diagram (PFD) will be constructed.
- The system will be simulated using LabVIEW™ control simulation software with the capability of simulating PID control of flow rate and pressure.
- After simulation, a user friendly control program will be programmed, which the user can modify for each experimental setup.
- After construction of the AMBSX, initial characterisation and calibration of the unit will be done including:
    - Total Internal volume
    - Flow rate calibration
    - Pressure and flow rate control and optimisation
    - General process accuracy and repeatability
- After initial characterisation and optimisation, a case study for the separation of Zr/Hf will be conducted, to validate the repeatability and accuracy of the design.

1.4. Outline and scope

In Chapter 2, a detailed literature survey on the membrane based extraction process is given, including detailed experimental setups that employ MBSX technology. It will also cover the programming language LabVIEW™, in which the control and monitoring of the AMBSX was done. In Chapter 3, the simulation of the control elements, namely flow rate and pressure, of the AMBSX are described using PID control and Cohen-Coon optimisation. The flow rate and pressure control of the system was simulated and described using the LabVIEW™ built-in control simulation function. In Chapter 4, the construction and automation of the AMBSX are described, including a repeatability case study that was conducted on the AMBSX. The first section includes a detailed PFD and parts list, including material selection. This will be followed by control and optimisation programming of the AMBSX. Lastly, a case study of the extraction of Zr/Hf to determine the stability and repeatability of the AMBSX is described. In the final chapter overall conclusions are drawn on the performance of the AMBSX, including recommendations for the further improvement of the AMBSX system.

This dissertation layout is as follows:

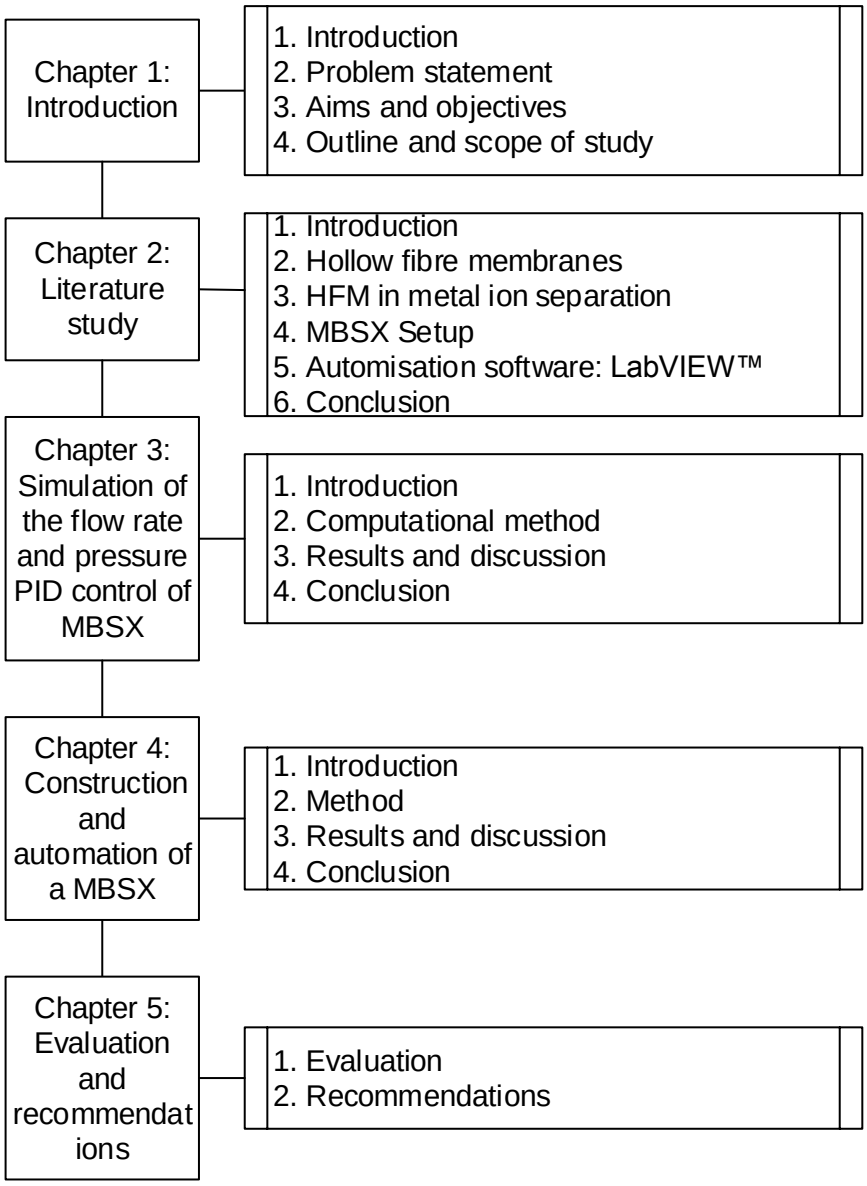

Figure 1-1: Dissertation layout

1.5. References

1. Sartori, E., *Nuclear data for radioactive waste management.* Annals of Nuclear Energy, 2013. **62**(0): p. 579-589.

2. Hallstadius, L., S. Johnson, and E. Lahoda, *Cladding for high performance fuel.* Progress in Nuclear Energy, 2012. **57**(0): p. 71-76.

3. Kirk, R.E. and D.F. Othmer, *Kirk-Othmer encyclopedia of chemical technology*. 1972: Interscience.

4. Collins, E.D., G.D. DelCul, B.B. Spencer, R.R. Brunson, J.A. Johnson, D.S. Terekhov, and N.V. Emmanuel, *Process Development Studies for Zirconium Recovery/Recycle from used Nuclear Fuel Cladding.* Procedia Chemistry, 2012. **7**(0): p. 72-76.

5. Steinbrück, M., *Hydrogen absorption by zirconium alloys at high temperatures.* Journal of Nuclear Materials, 2004. **334**(1): p. 58-64.

6. Zhou, B.X., M.Y. Yao, Z.K. Li, X.M. Wang, J. Zhou, C.S. Long, Q. Liu, and B.F. Luan, *Optimization of N18 Zirconium Alloy for Fuel Cladding of Water Reactors.* Journal of Materials Science & Technology, 2012. **28**(7): p. 606-613.

7. Smolik, M., A. Jakóbik-Kolon, and M. Porański, *Separation of zirconium and hafnium using Diphonix® chelating ion-exchange resin.* Hydrometallurgy, 2009. **95**(3–4): p. 350-353.

8. Kroschwitz, J.I. and Kirk-Othmer, *Kirk-Othmer Encyclopedia of Chemical Technology*. 2004: John Wiley & Sons.

9. Banda, R., H.Y. Lee, and M.S. Lee, *Separation of Zr from Hf in Hydrochloric Acid Solution Using Amine-Based Extractants.* Industrial & Engineering Chemistry Research, 2012. **51**(28): p. 9652-9660.

10. Banda, R. and M.S. Lee, *Solvent Extraction for the Separation of Zr and Hf from Aqueous Solutions.* Separation & Purification Reviews, 2014. **44**(3): p. 199-215.

11. Banda, R., S.H. Min, and M.S. Lee, *Selective extraction of Hf(IV) over Zr(IV) from aqueous H2SO4 solutions by solvent extraction with acidic organophosphorous based extractants.* Journal of Chemical Technology & Biotechnology, 2014. **89**(11): p. 1712-1719.

12. Reddy, B.R., J.R. Kumar, and A.V. Reddy, *Solvent extraction of zirconium(IV) from acid chloride solutions using LIX 84-IC.* Hydrometallurgy, 2004. **74**(1–2): p. 173-177.

13. Ritcey, G., *Solvent Extraction in Hydrometallurgy: Present and Future.* Tsinghua Science & Technology, 2006. **11**(2): p. 137-152.

14. Taghizadeh, M., R. Ghasemzadeh, S.N. Ashrafizadeh, K. Saberyan, and M.G. Maragheh, *Determination of optimum process conditions for the extraction and separation of zirconium and hafnium by solvent extraction.* Hydrometallurgy, 2008. **90**(2–4): p. 115-120.

15. van der Westhuizen, D.J., *Separation of Zirconium and Hafnium via Solvent Extraction*, in *Chemistry*. 2010, North-West University Potchefstroom. p. 141.

16. Law, J.D. and T.A. Todd, *Liquid-Liquid Extraction Equipment*. 2008, Idaho National Labratory

17. Kertész, R. and Š. Schlosser, *Design and simulation of two phase hollow fiber contactors for simultaneous membrane based solvent extraction and stripping of organic acids and bases.* Separation and Purification Technology, 2005. **41**(3): p. 275-287.

18. Gunderson, S.S., W.S. Brower, J.L. O'Dell, and E.N. Lightfoot, *Design of Membrane Cascades.* Separation Science and Technology, 2007. **42**(10): p. 2121-2142.

19. Boributh, S., W. Rongwong, S. Assabumrungrat, N. Laosiripojana, and R. Jiraratananon, *Mathematical modeling and cascade design of hollow fiber membrane contactor for CO2 absorption by monoethanolamine.* Journal of Membrane Science, 2012. **401–402**(0): p. 175-189.

20. Agarwal, S., M.T.A. Reis, M.R.C. Ismael, and J.M.R. Carvalho, *Zinc extraction with Ionquest 801 using pseudo-emulsion based hollow fibre strip dispersion technique.* Separation and Purification Technology, 2014. **127**: p. 149-156.

21. Rout, P.C. and K. Sarangi, *Separation of vanadium using both hollow fiber membrane and solvent extraction technique – A comparative study.* Separation and Purification Technology, 2014. **122**(0): p. 270-277.

22. Chaturabul, S., W. Srirachat, T. Wannachod, P. Ramakul, U. Pancharoen, and S. Kheawhom, *Separation of mercury(II) from petroleum produced water via hollow fiber supported liquid membrane and mass transfer modeling.* Chemical Engineering Journal, 2015. **265**: p. 34-46.

23. Wannachod, T., P. Phuphaibul, V. Mohdee, U. Pancharoen, and S. Phatanasri, *Optimization of synergistic extraction of neodymium ions from monazite leach solution treatment via HFSLM using response surface methodology.* Minerals Engineering, 2015. **77**(0): p. 1-9.

24. Fontàs, C., V. Salvadó, and M. Hidalgo, *Separation and Concentration of Pd, Pt, and Rh from Automotive Catalytic Converters by Combining Two Hollow-Fiber Liquid Membrane Systems.* Industrial & Engineering Chemistry Research, 2002. **41**(6): p. 1616-1620.

25. van der Westhuizen, D.J., G. Lachmann, and H.M. Krieg, *Method for selective separation and recovery of metal solutes from solution by the use of membrane based solvent extn*. 2012, North-West University, S. Afr p. 55pp.

26. Gabelman, A. and S. Hwang, *Hollow fiber membrane contactors.* Journal of Membrane Science, 1999. **159**(1–2): p. 61-106.

27. Gupta, S., M. Chakraborty, and Z.V.P. Murthy, *Performance study of hollow fiber supported liquid membrane system for the separation of bisphenol A from aqueous solutions.* Journal of Industrial and Engineering Chemistry, 2014. **20**(4): p. 2138-2145.

28. Shen, S.F., K.H. Smith, S. Cook, S.E. Kentish, J.M. Perera, T. Bowser, and G.W. Stevens, *Phenol recovery with tributyl phosphate in a hollow fiber membrane contactor: Experimental and model analysis.* Separation and Purification Technology, 2009. **69**(1): p. 48-56.

29. Wannachod, T., N. Leepipatpiboon, U. Pancharoen, and S. Phatanasri, *Mass transfer and selective separation of neodymium ions via a hollow fiber supported liquid membrane using PC88A as extractant.* Journal of Industrial and Engineering Chemistry, (0).

30. Williams, N.S., M.B. Ray, and H.G. Gomaa, *Removal of ibuprofen and 4-isobutylacetophenone by non-dispersive solvent extraction using a hollow fibre membrane contactor.* Separation and Purification Technology, 2012. **88**(0): p. 61-69.

31. Wongsawa, T., N. Sunsandee, U. Pancharoen, and A.W. Lothongkum, *High-efficiency HFSLM for silver-ion pertraction from pharmaceutical wastewater and mass-transport models.* Chemical Engineering Research and Design, (0).

CHAPTER 2: LITERATURE STUDY

2.1. Introduction

In this chapter a literature study is presented on topics related to the automation of a hollow fibre MBSX process. Firstly, different types of hollow fibre membranes and their applications and characteristics are presented. Subsequently, more detail is given on the use of hollow fibre membranes in metal ion extraction and the different configurations that can be used, including pertraction, supported hollow fibre extraction, and emulsified pertraction. This is followed by a brief overview of different MBSX setups used in literature, from which a general MBSX setup was derived. Finally, the automation hardware and software to be used in this study is described.

2.2. Hollow fibre membranes

In industrial applied SX, two immiscible liquids are dispersed into one another so that mass transfer can take place. This is normally achieved using SX equipment such as mixer-settlers, column contactors and centrifugal contactors. However, these dispersive techniques are inherently complex and introduce various problems into the process [1]. While the main aim in SX is to increase the contact area between the two liquids to increase the mass transfer between them, this can cause emulsification, foaming and flooding in mixer-settlers or column based contactors. In these systems it is also difficult to predict the mass transfer due to the complex fluid-dynamics involved. Other inherent problems include the large scale equipment needed, which consumes a large surface area of plant real-estate, as well as the dangers involved in open troughs with volatile solvents. However, for alternative technologies to compete with these existing techniques in view of the existing large investments, new technologies have to be low cost and environmentally friendly, while simultaneously increasing the efficacy and quality of the required products [2].

The use of membrane contactors in either flat sheet membrane or hollow fibre membrane modules has grown in popularity as a non-dispersive means of SX and has shown to be more effective than traditional mixer-settler contactors as the contact area of the liquids is both constant and gives a higher surface to volume area compared to dispersive SX techniques [3]. Since the contact is more constant, the predictability and modelling of hollow fibre extraction becomes easier with less complex fluid dynamic calculations [4]. Due to the lower contact surface area and lower volume throughput compared to a hollow fibre module contactor, flat sheet membrane contactors have to date mainly been used in laboratory scale experiments [5]. However, industrial scale membrane contactor plants that use hollow fibre membranes for waste water and off-gas treatment have been successfully implemented [6], confirming that this technology has the potential to be applied in numerous other industrial applications.

According to Gabelman and Hwang [2], advantages of using hollow fibre membranes include that the hollow fibre membrane contactor's surface areas are relatively large when compared to dispersive SX techniques, while not being affected by any differences in the flow rates of the two liquids as they are independent from one another. In addition, hollow fibre membranes stop the formation of undesirable 3rd phases or emulsions which can cause the entrainment of products [7]. The non-dispersive hollow fibre membrane technique allows the contacting of liquids with identical densities, which is not possible with traditional SX equipment [8]. Due to the design of the hollow fibre membrane contactors, the up-scaling to industrial size is linear, i.e. for larger volume applications additional modules are added in line. A hollow fibre membrane process can be run in continuous recirculation mode allowing equilibrium to be reached. In addition, when the extraction stage is coupled to a stripping stage, the product is simultaneously removed, avoiding any product inhibition effects [5]. Hollow fibre membrane kinetics are easier to predict and hence the process performance can be simulated with higher accuracy when compared to traditional SX techniques [9]. Hollow fibre membranes also have a low solvent and extractant loss, increasing lifetime and reducing costs. Lastly, hollow fibre membrane contactors have fewer mechanical parts than mixer-settlers, column contactors and centrifugal contactors, reducing the possibility of mechanical failures [2].

Gabelman and Hwang [2] also describe the disadvantages of hollow fibre contactors; the membrane module adds another resistance element in the flow line of a process, and in large scale operation MBSX will require additional pumps. Currently, baffles have been incorporated into the membrane contactor designs to reduce the amount of shell-side bypassing; however, this further increases the pressure loss across the membrane. Like all membrane processes, membrane contactors are susceptible to membrane fouling, while polymer dissolution could be caused by the organic solvents.

As the hollow fibre membrane is only the boundary support layer between the two phases, it plays no active role during extraction [10]. Hence the extraction is concentration driven, which differentiates this from other membrane applications such as water purification by reverse osmosis which is a pressure driven separation process. Being a physical phase separator, the polymer type of the membrane has no significant influence on the extraction, except for the wetting of the pores either by the organic or the aqueous stream, depending on whether the polymer is hydrophobic or hydrophilic. The materials used can, therefore, be adjusted to suit the chemical compatibility, as can be seen in literature where hollow fibre membranes have been made from polypropylene (PP), polyvinylidene fluoride (PVDF), perfluoroalkoxy alkanes (PFA) and polytetrafluoroethylene (PTFE) [5].

Hollow fibre membrane contactors have been commercially available since the 1980s, where they have initially been used in blood oxygenation devices and later for liquid degassing [5]. Membrana

is a recognized manufacturer of hollow fibre membrane contactors including the Celgard® Liqui-cel® brand of hollow fibre membranes. In this study, a hydrophobic membrane module from Membrana (Membrana Liqui-cel® Extra-Flow 2.5x8 X50) was used, where the 2.5 represents the internal diameter of the housing in inches, 8 refers to the fibre length in inches while X50 refers to the fibre type. Figure 2-1 displays parts of the external and internal structure of the contactor, consisting of a four port module. Two of the ports are inlets and two are outlets for the shell and lumen of the contactor, respectively. Both the module and the hollow fibre membranes are constructed from polypropylene, while the fibres are potted in polyethylene. The membrane has a surface contact area of 1.4 m^2 and a maximum liquid pressure and flow rate of 480 kPa and 11 L/min, respectively. The module also contains a baffle (not included in Figure 2-1) on the shell side to increase the liquid distribution within the module and thereby reducing shell side bypassing. A summary of the characteristics of the Liqui-cel® Extra-Flow 2.5x8 X50 membrane is presented in Table 2-1.

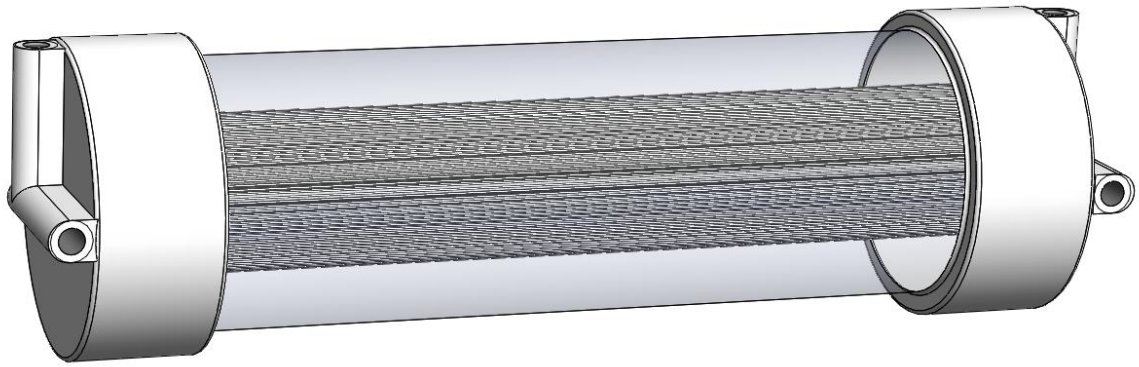

Figure 2-1: Schematic of a Liqui-cel® Extra-flow 2.5x8 hollow fibre membrane displaying a portion of the internal fibres [11]

Table 2-1: Liqui-cel® Extra-flow 2.5x8 X50 hollow fibre membrane characteristics [4,12,13]

Characteristic	Value
Module length (cm)	20.32
Module diameter (cm)	6.35
Housing material	Polypropylene
Fibre material	Polypropylene
Potting material	Polyethylene
Number of fibres	~10000
Fibre length (cm)	15.6
Fibre diameter (μm)	240
Fibre wall thickness (μm)	30
Pore size (μm)	0.03
Approximate surface area (m^3)	1.4

Hollow fibre membranes are used in various applications, for example for micro-extraction in analytical chromatography, by selectively extracting a compound before the sample is analysed [8,14-16]. Hollow fibre membranes are also used in industrial applications for the separation or removal of gasses such as carbon dioxide or oxygen, the degassing of liquids and removal of ammonia, removing pollutants from waste water streams, and metal ion extraction [17]. As this study will use the separation of Zr and Hf to illustrate the automation of the design, metal ion extraction applications of hollow fibre membranes will be discussed in more detail.

2.3. Hollow fibre membranes in metal ion SX

As discussed above, pertraction is a technique where two liquids are contacted over a hollow fibre membrane. In the pertraction configuration, where the extraction and stripping are completed independently [8,12,18], an aqueous feed stream in which the metal salts are dissolved in an acid medium, is contacted with the organic phase, which consists of the extractant, the diluent and a modifier. The subsequent stripping of the loaded organic phase can be done in two different configurations as illustrated in Figure 2-2. In setup (A), a single membrane is used. Firstly, the aqueous feed is extracted until the organic phase has reached equilibrium. Then the aqueous tank is replaced with stripping liquor and the loaded organic is stripped. In setup (B), a second membrane contactor is utilised and the organic feed is circulated through both membranes, thus simultaneous loading and stripping occurs. This will reduce effects such a product inhibition while maintaining a high concentration gradient.

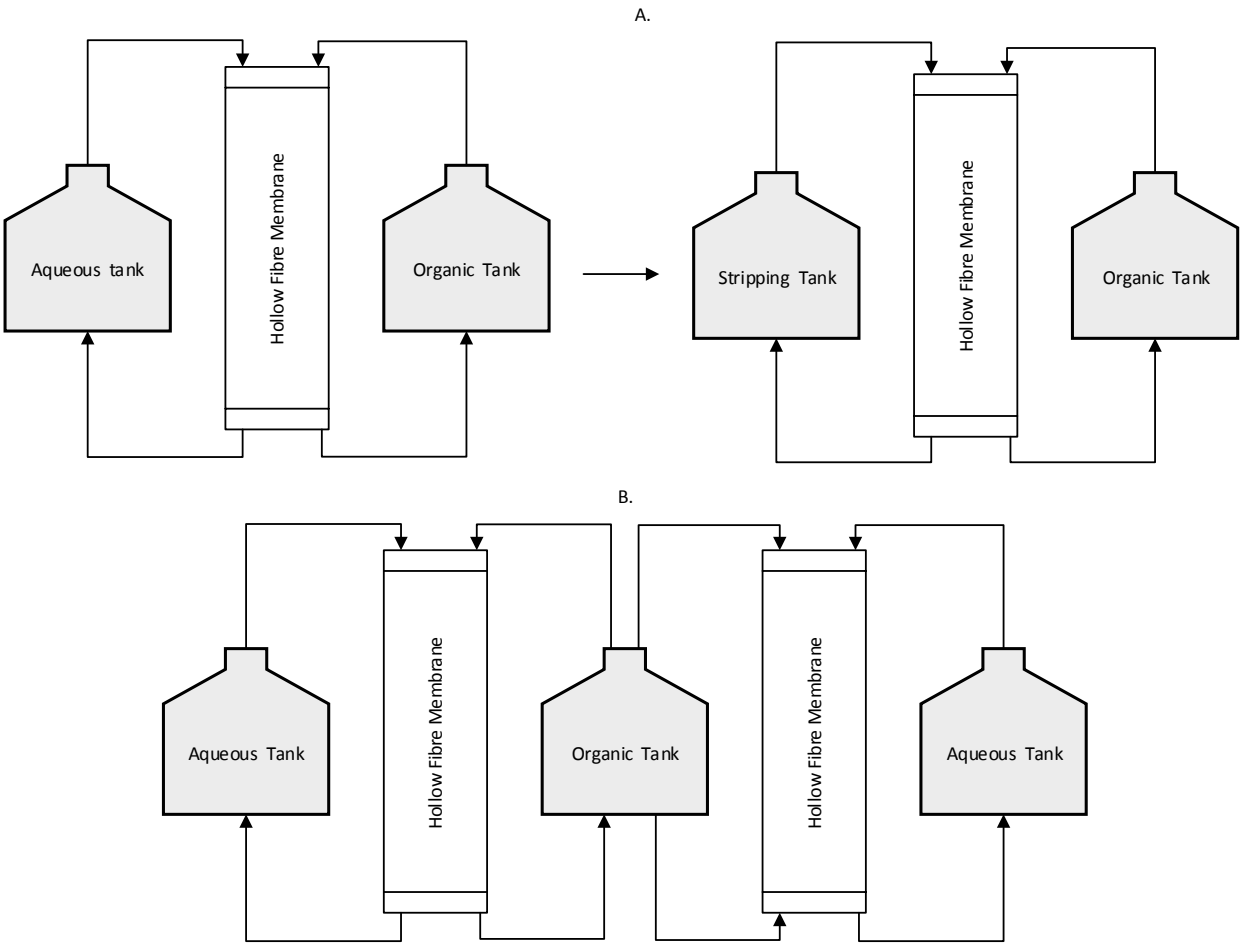

Figure 2-2: (A) Schematic of separate hollow fibre pertraction and stripping setup. (B) Schematic of pertraction with simultaneous stripping.

An additional technique of hollow fibre membrane extraction includes hollow fibre supported liquid membranes (HFSLM) [7,9,19,20]. In HFSLM the extractant is immobilised in the pores of the hollow fibre by capillary forces due to the hydrophobic properties of the hollow fibre membrane [21]. The aqueous feed and stripping liquor are then circulated through the shell and lumen. This technique has the benefit that the extraction and stripping occur in a single step, which reduces cost, as only enough extractant is needed for the doping of the pores of the hollow fibre membranes. However, disadvantages of this configuration include extractant loss at high flow rates while the doping of the membrane changes the process to a more batch type process [15].

Another method used for metal ion extraction is hollow fibre emulsified pertraction where the strip phase is emulsified in the extractant and both are simultaneously contacted with the aqueous feed phase through the hollow fibre membranes [6,13,22], also resulting in a single extracting and stripping step. Emulsified pertraction has shown to be effective when the concentration of the metal in the feed stream is below 0.1 g/L [23]. However, this technique reintroduces the problem of 3rd phase formation which was one of the reasons for the introduction of the hollow fibre membranes in the first place.

MBSX has been used extensively in metal ion extraction studies including transition metals [13,23,24], heavy metals [25,26], platinum group metals [27,28] and rare earth metals [19]. In view of the scope for this study, the focus in this discussion will be on Zr and Hf separation. The separation of Zr and Hf using MBSX was illustrated by Yang et al. [15,16], where a HFSLM was used to separate Zr and Hf as a preconditioning step for a chromatographic analysis. In their study, a trace Zr/Hf mixture was separated using a tri-n-octyl-monomethyl ammonium chloride (Aliquat 336) as extractant in a hydrochloric acid medium. A selective extraction of Zr (85%) and Hf (15%) was obtained. The parameters that influenced the extraction and separation were the flow rates of the feed and striping liquor, while factors affecting the extraction were the fibre length and flow rates. In 2012, van der Westhuizen et al. [29] filed a patent that describes the MBSX method for the selective separation of metals, including the separation of Zr and Hf, from aqueous solutions. According to the patent, a manually operated MBSX setup is used in the selective extraction of Zr from Hf using emulsified pertraction on a Zr/Hf oxy-chloride salt in a nitric acid medium with Aliquat 336 as the extractant. The experimental setup involved a Liqui-cel® Extra-Flow 2.5x8 X50 hollow fibre membrane in an experimental setup as illustrated in Figure 2-3. The setup used in the patent will form the basis of this study, in which the manually controlled MBSX will be automated and optimised for the extraction and separation of Zr and Hf.

2.4. MBSX experimental setup

For many of the metal extractions, as well as for the removal of organic compounds from waste streams and micro-extraction analysis techniques, a similar setup to the one presented in Figure 2-3 has been used [8,30-32]. However, all the setups presented in literature have been manually controlled. According to literature [8,30-32] , most setups consist of a storage tank for the aqueous, organic feed and stripping liquor (if simultaneous stripping is performed). The inlet and outlet pressures are typically metered with a needle gauge and flow is monitored and controlled with a manual flow gauge. The pumps of these setups consist of either peristaltic or gear drive pumps. Figure 2-3 shows a PFD constructed of the representative MBSX experimental setup obtained from literature. The lack of any automation or data logging apparatus suggests a gap where further improvements in the MBSX technology can be achieved. By automating the MBSX setup, accuracy of measurements and control of the system can be better managed while the data collection and logging can provide more data to help improve the understanding of the system. In addition, further monitoring elements such as temperature monitoring of feed tanks, as well as digital pressure and flow meters that can give a higher degree of accuracy can be added. Coupling all control and measurement elements to a central controller would also allow for the automation of the process allowing the MBSX studies to be more consistent with a higher repeatability between runs.

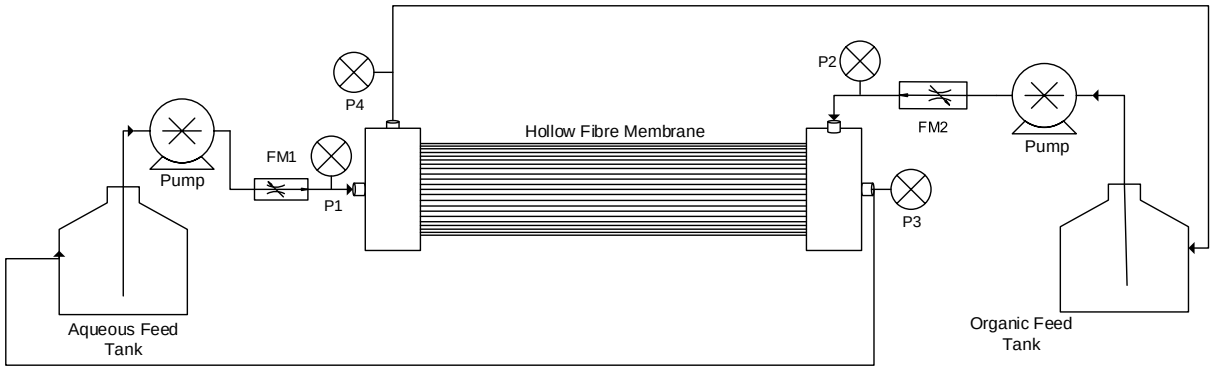

Figure 2-3: Generalised PFD of a manually controlled MBSX setup derived from literature [8,30-32]

2.5. Automisation software: LabVIEW™

As the main objective of this study was to automate the MBSX process, possible options for supplying hardware and software to automate such a process should be considered. A common type of automation hardware is the programmable logic controller (PLC). PLC's replaced the previous forms of automation that consisted of using relays and timing belts [33]. According to Fauci [34], distributed control systems (DCS) started gaining popularity; they had the advantage of being centralised, allowing for plant wide control from a central point. However, as both technologies have improved, the differences between PLC and DCS became smaller and they now preform similarly and it has become difficult to differentiate between the two types of architecture. A DCS type of automation system is the National Instruments (NI) configurable embedded control system with the programming software LabVIEW™. NI systems have the advantage of working with configurable input and output (I/O) modules that can be customised to suit the process needs that integrate seamlessly into the programming language [35-38]. LabVIEW™ is a graphical flowchart style of programming language that has aimed to simplify data acquisition and device automation for the last three decades since its debut in 1986. LabVIEW™ is an acronym for Laboratory Virtual Instrument Engineering Workbench, which in fact suggests the main application of the LabVIEW™ environment. LabVIEW™, when coupled with interface modules or standard input output communication protocols, such as RS232 or Ethernet, is able to measure or control any device that uses these communication protocols [39]. LabVIEW™ has been developed to run as standalone devices, or as complex embedded control systems and has the capability to simulate these devices so that programming and optimisation can be simulated before being implemented in the actual devices [40].

Over the years, NI has developed a central point control system that could connect multiple devices from different manufacturers that will be controlled by one program, effectively making it a virtual instrument. LabVIEW™'s graphical interface has two distinct sections, namely the front panel and the block diagram. The front panel, an example of which is displayed in Figure 2-4, is

where the user interface (UI) is programmed and controlled. When operating the device, the operator will see the front panel, which includes all the controls that the operator can change such as buttons, switches and input boxes. The front panel can also display data acquired in real time by means of graphs, charts or tables.

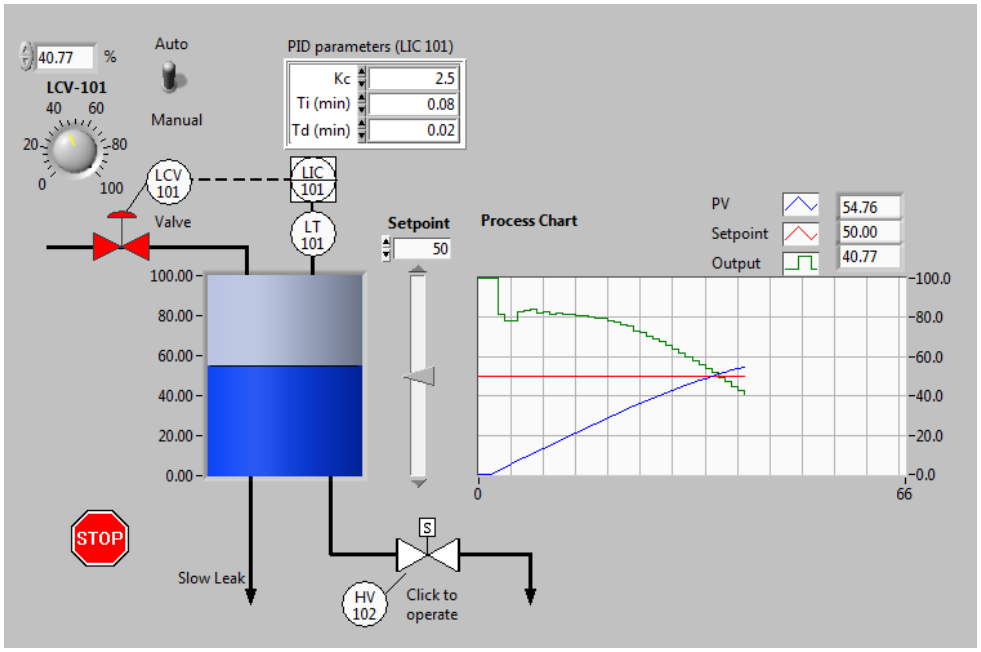

Figure 2-4: Example of LabVIEW™ front panel (obtained from NI LabVIEW example documentation) [41]

The block diagram part of a LabVIEW™ program, as seen in Figure 2-5, is where all the programming is done. It works in a flow diagram mechanism, where variables or functions are connected by data wires. The flow diagram programming is read in a left-to-right direction. This type of programming allows for complex codes to be applied in a simplified manner compared to many lines of code that would be required in typical text based coding [35]. The flow diagram also uses multithreaded process programming, which allows the program to complete multiple tasks simultaneously.

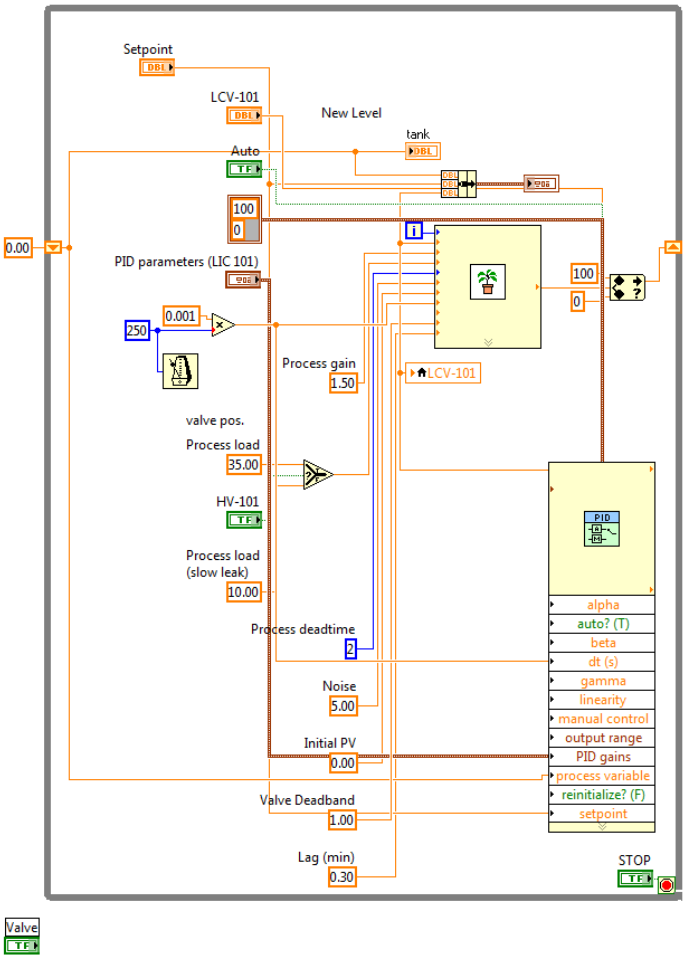

Figure 2-5: Example of LabVIEW™ block diagram (obtained from NI LabVIEW example documentation) [41]

LabVIEW™ has been developed for the data acquisition and control of devices and is supported by NIs large array of devices aimed at connecting devices so that LabVIEW™ can be used to monitor or control these devices. National Instrument's range of data acquisition devices are modular in design and can thus be specifically fitted with the modules required to control or monitor the specified equipment [42]. Hence connecting devices to a LabVIEW™ program is as simple as a drag and drop of the required instrument variable into the block diagram.

NIs range of embedded control systems include a high speed data acquisitions system, named Compaq-RIO, which contains a FPGA (field-programmable gate array) processor that allows the control program to be loaded on the Compaq-RIO internal storage, allowing the system to acquire data at higher rates (up to 800 000 samples per second) and to run independently from the control computer [43]. This is necessary when devices must be read at high speed for example when using a square wave pulse generation detector that is used in metering devices such a turbine flow meters.

2.6. Conclusion

Measured in terms of the increase of publications in the last two decades, an increase in research interest in the field of hollow fibre membranes can be seen. This interest, especially in terms of metal ion separation, has brought about a novel hydrometallurgical separation technique that can be applied for a wide range of metals, from transition to rare earth metals. Literature reports three techniques used in hollow fibre membrane extraction, and it can be concluded that, while pertraction requires either a two-step or a two membrane system, it has increased stability and repeatability compared to traditional SX processes. Literature outlines a standard hollow fibre extraction experimental setup; however, this setup is analogically controlled, which increases the difficulty of repeatability and data logging. No research in the automation of hollow fibre membrane pertraction systems were found in literature. It was determined that automation will benefit the hollow fibre extraction studies by increasing control and monitoring of the system, which has been lacking in previous studies. The hardware and software used in the automation of laboratory equipment was described and it was found that NI' LabVIEW™ was the forerunner in automation research, due to its modular form and ease of use while the flow chart style of programming has been successfully implemented in laboratory scale to industrial scale processes.

2.7. References

1. Law, J.D. and T.A. Todd, *Liquid-Liquid Extraction Equipment*. 2008, Idaho National Labratory

2. Gabelman, A. and S. Hwang, *Hollow fiber membrane contactors.* Journal of Membrane Science, 1999. **159**(1–2): p. 61-106.

3. Soldenhoff, K., M. Shamieh, and A. Manis, *Liquid–liquid extraction of cobalt with hollow fiber contactor.* Journal of Membrane Science, 2005. **252**(1–2): p. 183-194.

4. Rout, P.C. and K. Sarangi, *Comparison of hollow fiber membrane and solvent extraction techniques for extraction of cerium and preparation of ceria by stripping precipitation.* Journal of Chemical Technology and Biotechnology, 2014.

5. Pabby, A.K. and A.M. Sastre, *State-of-the-art review on hollow fibre contactor technology and membrane-based extraction processes.* Journal of Membrane Science, 2013. **430**: p. 263-303.

6. Klaassen, R., P.H.M. Feron, and A.E. Jansen, *Membrane Contactors in Industrial Applications.* Chemical Engineering Research and Design, 2005. **83**(3): p. 234-246.

7. Wongsawa, T., N. Sunsandee, U. Pancharoen, and A.W. Lothongkum, *High-efficiency HFSLM for silver-ion pertraction from pharmaceutical wastewater and mass-transport models.* Chemical Engineering Research and Design, (0).

8. Shen, S.F., K.H. Smith, S. Cook, S.E. Kentish, J.M. Perera, T. Bowser, and G.W. Stevens, *Phenol recovery with tributyl phosphate in a hollow fiber membrane contactor: Experimental and model analysis.* Separation and Purification Technology, 2009. **69**(1): p. 48-56.

9. Bringas, E., M.F. San Román, J.A. Irabien, and I. Ortiz, *An overview of the mathematical modelling of liquid membrane separation processes in hollow fibre contactors.* Journal of Chemical Technology and Biotechnology, 2009. **84**(11): p. 1583-1614.

10. Gawroński, R. and B. Wrzesińska, *Kinetics of solvent extraction in hollow-fiber contactors.* Journal of Membrane Science, 2000. **168**(1–2): p. 213-222.

11. *2.5 X 8 EXTRAFLOW, CLAMPED* [Mechanical Drawing] 2006 26/04/2012 [cited 2015 08/10/2015]; Available from: http://www.liquicel.com/uploads/documents/2.5%20x%208%20Clamped%20with%20NPT%20ports%2012-2837%20rev4.pdf.

12. Williams, N.S., M.B. Ray, and H.G. Gomaa, *Removal of ibuprofen and 4-isobutylacetophenone by non-dispersive solvent extraction using a hollow fibre membrane contactor.* Separation and Purification Technology, 2012. **88**(0): p. 61-69.

13. Agarwal, S., M.T.A. Reis, M.R.C. Ismael, and J.M.R. Carvalho, *Zinc extraction with Ionquest 801 using pseudo-emulsion based hollow fibre strip dispersion technique.* Separation and Purification Technology, 2014. **127**: p. 149-156.

14. Esrafili, A., Y. Yamini, M. Ghambarian, M. Moradi, and S. Seidi, *A novel approach to automation of dynamic hollow fiber liquid-phase microextraction.* J. Sep. Sci., 2011. **34**(8): p. 957-964.

15. Yang, X.J., A.G. Fane, and C. Pin, *Separation of zirconium and hafnium using hollow fibers: Part I. Supported liquid membranes.* Chemical Engineering Journal, 2002. **88**(1–3): p. 37-44.

16. Yang, X.J., A.G. Fane, and C. Pin, *Separation of zirconium and hafnium using hollow fibres: Part II. Membrane chromatography.* Chemical Engineering Journal, 2002. **88**(1–3): p. 45-51.

17. *About Liqui-Cel Membrane Gas Transfer Devices*. 2015 [cited 2015 05/10/2015]; Available from: http://www.liquicel.com/about.cfm.

18. Fadaei, F., S. Shirazian, and S.N. Ashrafizadeh, *Mass transfer simulation of solvent extraction in hollow-fiber membrane contactors.* Desalination, 2011. **275**(1-3): p. 126-132.

19. Wannachod, T., P. Phuphaibul, V. Mohdee, U. Pancharoen, and S. Phatanasri, *Optimization of synergistic extraction of neodymium ions from monazite leach solution treatment via HFSLM using response surface methodology.* Minerals Engineering, 2015. **77**(0): p. 1-9.

20. San Román, M.F., E. Bringas, R. Ibañez, and I. Ortiz, *Liquid membrane technology: Fundamentals and review of its applications.* Journal of Chemical Technology and Biotechnology, 2010. **85**(1): p. 2-10.

21. Kocherginsky, N.M., Q. Yang, and L. Seelam, *Recent advances in supported liquid membrane technology.* Separation and Purification Technology, 2007. **53**(2): p. 171-177.

22. Sonawane, J.V., A.K. Pabby, and A.M. Sastre, *Pseudo-emulsion based hollow fibre strip dispersion (PEHFSD) technique for permeation of Cr(VI) using Cyanex-923 as carrier.* Journal of Hazardous Materials, 2010. **174**(1–3): p. 541-547.

23. Ganesh Prasadh, K., S. Venkatesan, K.M. Meera Sheriffa Begum, and N. Anantharaman, *Emulsion Liquid Membrane Pertraction of Zinc and Copper: Analysis of Emulsion Formation using Computational Fluid Dynamics.* Chemical Engineering & Technology, 2007. **30**(9): p. 1212-1220.

24. Rout, P.C. and K. Sarangi, *Separation of vanadium using both hollow fiber membrane and solvent extraction technique – A comparative study.* Separation and Purification Technology, 2014. **122**(0): p. 270-277.

25. Yun, C.H., R. Prasad, A.K. Guha, and K.K. Sirkar, *Hollow fiber solvent extraction removal of toxic heavy metals from aqueous waste streams.* Industrial & Engineering Chemistry Research, 1993. **32**(6): p. 1186-1195.

26. Chaturabul, S., W. Srirachat, T. Wannachod, P. Ramakul, U. Pancharoen, and S. Kheawhom, *Separation of mercury(II) from petroleum produced water via hollow fiber supported liquid membrane and mass transfer modeling.* Chemical Engineering Journal, 2015. **265**: p. 34-46.

27. Fontàs, C., V. Salvadó, and M. Hidalgo, *Separation and Concentration of Pd, Pt, and Rh from Automotive Catalytic Converters by Combining Two Hollow-Fiber Liquid Membrane Systems.* Industrial & Engineering Chemistry Research, 2002. **41**(6): p. 1616-1620.

28. Harjanto, S., Y. Cao, A. Shibayama, I. Naitoh, T. Nanami, K. Kasahara, Y. Okumura, K. Liu, and T. Fujita, *Leaching of Pt, Pd and Rh from Automotive Catalyst Residue in Various Chloride Based Solutions.* Materials Transactions, 2006. **47**(1): p. 6.

29. van der Westhuizen, D.J., G. Lachmann, and H.M. Krieg, *Method for selective separation and recovery of metal solutes from solution by the use of membrane based solvent extn*. 2012, North-West University, S. Afr p. 55pp.

30. Trivunac, K., S. Stevanovic, and M. Mitrovic, *Pertraction of phenol in hollow-fiber membrane contactors.* Desalination, 2004. **162**(0): p. 93 - 101.

31. Kertész, R., M. Šimo, and Š. Schlosser, *Membrane-based solvent extraction and stripping of phenylalanine in HF contactors.* Journal of Membrane Science, 2005. **257**(1–2): p. 37-47.

32. Kertész, R. and Š. Schlosser, *Design and simulation of two phase hollow fiber contactors for simultaneous membrane based solvent extraction and stripping of organic acids and bases.* Separation and Purification Technology, 2005. **41**(3): p. 275-287.

33. Svrcek, W.Y., D.P. Mahoney, and B.R. Young, *A real-time approach to process control*. 2006: Wiley.

34. Fauci, J.L., *PLC or DCS: selection and trends.* ISA Transactions, 1997. **36**(1): p. 21-28.

35. Wagner, C., S. Armenta, and B. Lendl, *Developing automated analytical methods for scientific environments using LabVIEW.* Talanta, 2010. **80**(3): p. 1081-1087.

36. Mingle, Z., Y. Jintian, J. Guoguang, and L. Gang, *System on Temperature Control of Hollow Fiber SpinningMachine Based on LabVIEW.* Procedia Engineering, 2012. **29**(0): p. 558-562.

37. Klocke, F., O. Dambon, U. Schneider, R. Zunke, and D. Waechter, *Computer-based monitoring of the polishing processes using LabView.* Journal of Materials Processing Technology, 2009. **209**(20): p. 6039-6047.

38. Johnson, B.N. and N. Sobel, *Methods for building an olfactometer with known concentration outcomes.* Journal of Neuroscience Methods, 2007. **160**(2): p. 231-245.

39. Elliott, C., V. Vijayakumar, W. Zink, and R. Hansen, *National Instruments LabVIEW: A Programming Environment for Laboratory Automation and Measurement.* Journal of the Association for Laboratory Automation, 2007. **12**(1): p. 17-24.

40. Gutiérrez-Castrejón, R. and M. Duelk, *Using LabVIEW™ for advanced nonlinear optoelectronic device simulations in high-speed optical communications.* Computer Physics Communications, 2006. **174**(6): p. 431-440.

41. National Instruments, *LabVIEW™ 2011 Example Programs* in *Simulation -Tank Level.vi*. 2011.

42. Shukor, S.R.A., R. Barzin, and A.L. Ahmad, *Computer-Based Control for Chemical Systems Using LabVIEW® in Conjunction with MATLAB®*, in *Practical Applications and Solutions Using LabVIEW™ Software*, S. Folea, Editor. 2011, InTech. p. 14.

43. Wu, B., V. Yufit, J. Campbell, G.J. Offer, R.F. Martinez-Botas, and N.P. Brandon. *Simulated and experimental validation of a fuel cell-supercapacitor passive hybrid system for electric vehicles*. in *Hybrid and Electric Vehicles Conference 2013 (HEVC 2013), IET*. 2013.

CHAPTER 3: SIMULATION OF THE FLOW RATE AND PRESSURE PID CONTROL OF AN MBSX

3.1. Introduction

The separation of Zr from Hf is essential for the production of cladding material for nuclear fuel rods. The Zr alloy is used for its high melting point, low hydrogen absorption and low thermal neutron capture absorption cross-section [1]. Zircon ores are typically contaminated with 1-3% Hf, which has a high thermal neutron absorption cross-section of approximately 600 times that of Zr. This contamination increases the neutron absorption in the alloy, diminishing the performance of the alloy and hence needs to be separated from the Zr. The production of nuclear grade Zr that has less than 100ppm Hf contamination is an intricate and costly process since Zr and Hf have very similar physical and chemical properties making their separation difficult [2]. SX has been identified as a potential technique for the separation and purification of these metals [3-5], as discussed in Chapter 2.

While SX of Zr from Hf shows potential as an effective separation method which could produce nuclear grade Zr [3-5], traditional SX has some disadvantages, most importantly the contact of organic and aqueous layers leading to the formation of emulsions, which trap the metals in a third phase, reducing the effectivity of the extraction process. An alternative approach that avoids this shortfall is the MBSX process [6-8]. During MBSX the organic phase is immobilised in the pores of a hydrophobic hollow fibre membrane. This creates a contacting surface point at the membrane pores, allowing mass transfer to take place without mixing of the two phases, removing the possibility of emulsification [9].

A schematic representation of a manually operated MBSX unit, adapted from [7,10,11], is shown in Figure 2-3. To date this setup was manually controlled by varying the inlet and outlet pressures by adjusting i) the rotation speed of the gear pumps and ii) the flow meters to obtain the desired flow rates and pressures. For MBSX the internal liquid pressure of the aqueous phase must be higher than that of the organic phase to retain the organic-phase and ensure no cross-over through the hydrophobic fibres. However, this difference in pressure must not exceed the breakthrough pressure, when transfer of the aqueous phase into the organic phase will occur, hence accurate control of flow rate and pressures is crucial [12].

While this original setup was sufficient for the initial studies, its manual input made control and repeatability difficult, giving rise to the need for an automated unit. The experimental variables must be controlled by a single control program, called a virtual instrument (VI), to incorporate all measurements and control the MBSX in one program that can monitor and control the temperature, differential pressure and flow rate. The program must also record experimental descriptions including metal salt, acid and additives, type and concentrations for the aqueous side; and extractant, diluent and modifier type and concentration for the organic phase. To attain this, LabVIEW software, which has been designed by NI, was used [13]. LabVIEW is used in

conjunction with NI modular control units, which connect the computer to peripheral devices that acquire and generate digital and analogue signals including voltage resistance and current signals. The control program allows the process kinetics to be studied and optimised, thus aiding the Zr and Hf separation research. In this study the graphical user interface (GUI) of the MBSX program was designed and a control program, which controlled the pressure and flow rate, was simulated and optimised for the automated MBSX system. This was achieved by simulating process conditions using LabVIEW simulation and PID control packages. The control program was programmed using PID control and optimisation was done by tuning the PID with a combination of trial and error and Cohen-Coon tuning methods [14].

3.2. Computational method

The control program consisted of a GUI which allowed the operator to enter and view details and parameters of the MBSX. The GUI was split into four individual tabs. In the Operator and Experimental details tab, the operator needed to enter all required data for data logging purposes. The Experimental parameter tab displayed all the switches and input boxes for the set values required for the program to control the MBSX including set temperature, pressure flow rate and run time. It also included the current flow and pressure. On the last two tabs the real time data was obtained and plotted including the current pressure, temperature and flow rate, which was displayed in chart and table form to be exported to 3rd party data analysis software.

The automated MBSX was based on the design of the manual system. The main variables that were required to control the system were pressures and flow rates. These variables needed to be independently adjustable; however, changing the values of either directly impacts the other as they are fundamentally related in a closed system. The flow rate of the liquids was controlled by changing the rotational speed of the gear drive pumps that were coupled to a turbine flow sensor, allowing for accurate measuring of the flow rate entering the membrane module, whilst the internal liquid pressure was controlled via an electronically actuated control valve located after the membrane module. The pressure was measured via digital pressure transmitters located before and after the membrane module to measure the pressure differential.

NI LabVIEW uses two interfaces namely a front panel and a block diagram. The front panel is visible to the operator of the MBSX and includes inputs and outputs of the MBSX program. The front panel allows the operator to control all aspects of information and control options for the MBSX. The rear block diagram is the area where all the programming is done by means of a block and wire graphical programming style. Each block represents a component or function that is connected in logical order with wires [13].

A simulation of the control of the MBSX unit was programmed using LabVIEW internal simulation and PID functionality. As mentioned earlier, the flow rate and pressure of the system needs to be independently controlled, yet they are fundamentally linked and therefore a control program is needed, to be able to independently control the flow rate and pressure. Two PID control systems were used as the control algorithm for the flow control and the pressure control. The PID's are optimised by varying the three parameters which are the proportional gain Kc, integral time T_i and derivative time T_d. A flow rate PID was programmed by an initial simulated ramp signal that was linked to a sub program that forms part of the LabVIEW package called "Plant simulator.vi". This subprogram simulates a process plant, in this case a pump, allowing characteristics such as gain, noise, dead time and lag of that system to be simulated. The PID-controller controls the flow rate by adjusting the pump revolution speed, with each revolution pumping a known volume of liquid. The PID for flow rate must have a slow response time with no overshoot to counter any sudden pressure spikes in the closed system. After the flow rate was simulated, the internal liquid pressure was calculated by solving the Van Der Waals Equation [15], shown in Equations 1 and 2.

$$\left(p + \frac{n^2 a}{V^2}\right)(V - nb) = nRT, \qquad [1]$$

Written in terms of pressure (p):

$$p = \frac{nRT}{(V - nb)} - \left(\frac{n^2 a}{V^2}\right) \qquad [2]$$

where R is the universal gas constant (8.314 J/mol.K), V is total internal volume (m^3), n is the number of molecules (mol), T is the temperature (K), a is the measure of attraction between particles ($J.m^3/mol^2$), and b the volume excluded by a mole of particles (m^3/mol). The pressure was then controlled by a PID-controller on a control valve that adjusts the pressure by opening or closing its orifice. As the pressure PID system is dependent on the flow rate, a fast responding PID is needed. However, a noisy signal was observed and hence a low-pass filter was added to reduce the noise. The flow rate PID was optimised by applying the Cohen-Coon tuning method, which is described in detail by Svrcek et al. [14]. Initially the PID variables were minimised manually so that a steady-state signal with no oscillations was achieved. After the steady state was reached, the set point was changed and the change in process reaction curve recorded. The reaction curve allowed the process parameters to be calculated, namely M, the change of input (%); N, the change in process variable (%); L, the delay time (min) for a change in process variable after a change in set point; R, the lag ratio, which was obtained by dividing the L by the time taken

(min) to achieve 63% change in the process variable. Once this data have been obtained, it was applied to the Cohen-Coon tuning equations for proportional only (P), proportional integral (PI) or proportional integral derivative (PID) control as seen in Table 3-1. After the Cohen-Coon tuning, further fine tuning was done using a trial and error method. The trial and error method involves changing the P, PI and PID variables in small increments to achieve desired control results.

Table 3-1: Cohen-Coon tuning equations

	K_c	T_i	T_d
P	$\frac{M}{NL}(1+\frac{R}{3})$	0	0
PI	$\frac{M}{NL}(0.9+\frac{R}{12})$	$L(\frac{30+3R}{9+20R})$	0
PID	$\frac{M}{NL}(1.33+\frac{R}{4})$	$L(\frac{32+6R}{13+8R})$	$L(\frac{4}{11+2R})$

3.3. Results and discussion

The main GUI, as seen in Figure 3-1, was developed to be user friendly and incorporates convenient features while displaying all relevant information to the operator. The GUI was split into four different tabs, i.e. User Input, Procedure, Data Logs and Data Tables. The User Input tab included Operator and membrane details and described both aqueous and organic liquid phases' compositions. The interface allowed all relevant information to be displayed simultaneously to the operator, yet split into different windows to allow for easy navigation. The programming block diagram for the UI and PID control can be seen in Figure 3-2.

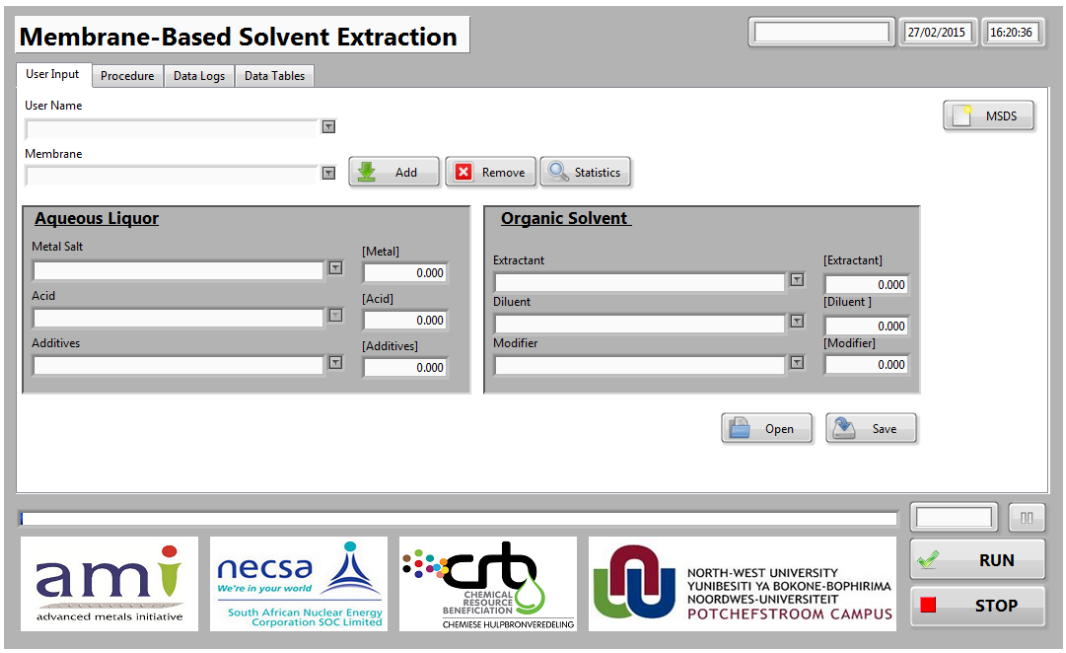

Figure 3-1: GUI displaying the User Input Tab

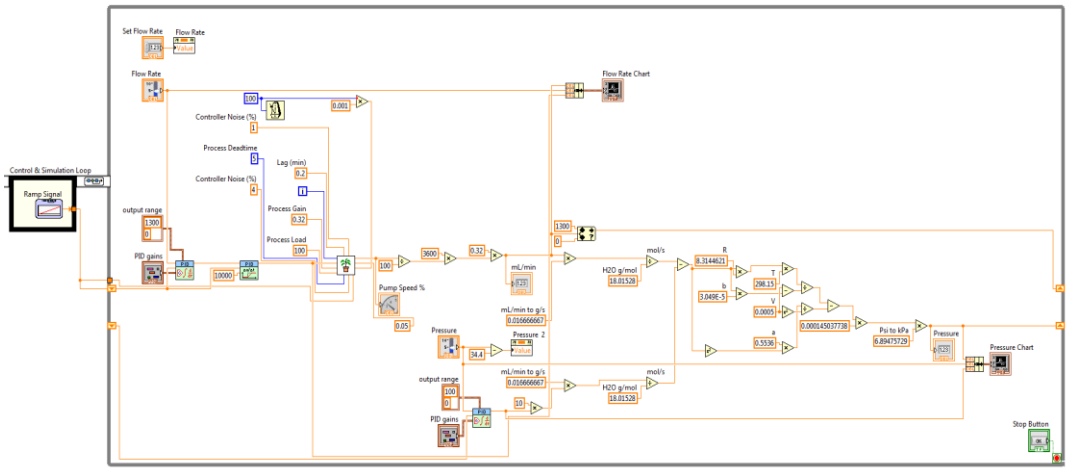

Figure 3-2: PID for flow rate and pressure LabVIEW code

The control of flow rate and pressure was simulated using the built in PID function and optimised using the Cohen-Coon and the trial and error tuning methods. The tuning variables K, T_i and T_d were calculated for each model using the Cohen-Coon method and are displayed in Table 3-2. The P, PI, PID and PID with fine tuning were applied the flow rate and plotted in Table 3-2.

From Figure 3-3 it can be seen that P control gave a large overshoot, which is not desirable as it will cause increased pressure over the system. PID control was suitable as a control algorithm; however, PID is not preferred in closed flow control systems as it yields inherently noisy signals that increase the wear of the control equipment [14]. PI was therefore chosen for further fine

tuning. It can be seen that, after fine tuning, there was neither overshoot nor oscillations and that the system achieved steady-state within 12 seconds from a disturbance.

Table 3-2: Cohen-Coon tuned PID variable results

	K	T_i (min)	T_d (min)
P	4.6712	0	0
PI	3.9874	0.0681	0
PID	6.0194	0.0679	0.0105

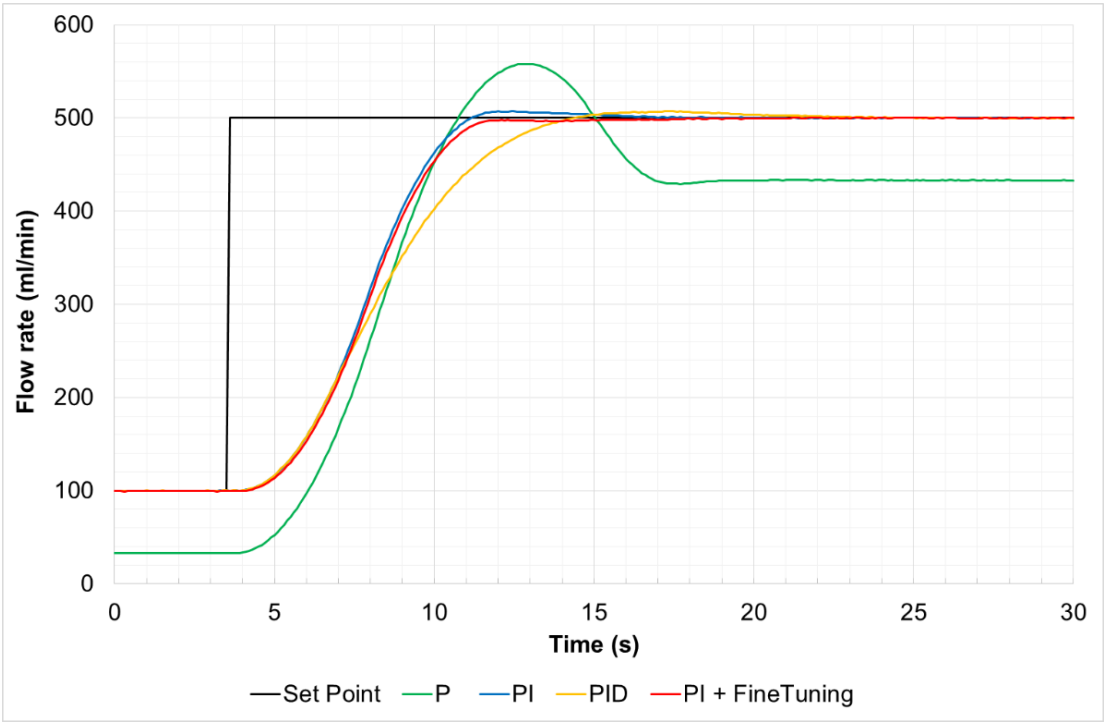

Figure 3-3: Cohen-Coon tuning of flow rate

After fine tuning the PI flow rate, the variable values of $K_c = 4.1658$ and $T_i = 0.0716$ min gave the best control by obtaining equilibrium with no overshoot or oscillation. The tuning of the pressure PI could not be achieved using Cohen-Coon as the signal noise did not allow the signal to achieve coherent oscillations and hence it was tuned only by the trial and error method. Using this approach, an optimal control was observed with $K_c = -0.0112$ and $T_i = 0.00034$ min as it gave the quick response required for the pressure control. The pressure PI-controller was optimised to ensure that a change in flow rate would not exceed 10% above the set point of the pressure if a disturbance in flow occurred. This was tested and displayed in Figure 3-4.

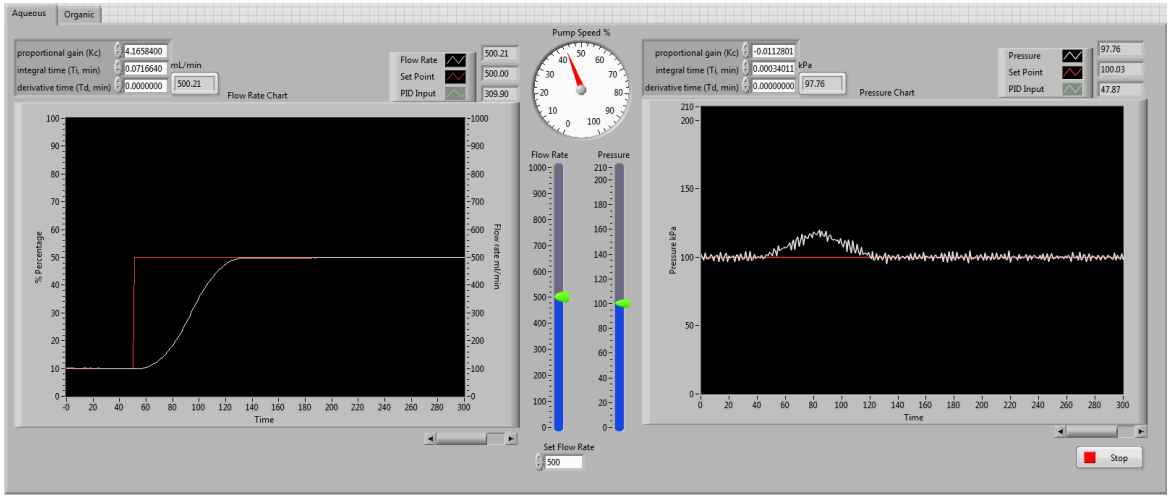

Figure 3-4: Control GUI for flow rate and pressure of the MBSX system, with a disturbance in flow rate and the effect on pressure

3.4. Conclusion

In this study it was shown how a GUI of an automated MBSX instrument can be simulated using the NI LabVIEW program. A proof of concept simulation of the control of flow rate and pressure of a closed system was achieved via PI control of the pump and control valves in the MBSX system. The flow rate PI controller was tuned using the Cohen-Coon method and fine-tuned using the trial and error method while the pressure PI was manually tuned using only the trial and error method. Using the optimised system, steady state was achieved after an average of 12 seconds from a disturbance of flow rate, while steady state of pressure was attained after 7 seconds from a disturbance. PI parameters were optimised at $K_c = 4.1658$ and $T_i = 0.0716$ min for the flow rate and $K_c = -0.0112$ and $T_i = 0.00034$ min for the pressure. The flow rate PI had to be adjusted with a slow response to counteract any over-pressures forming when the pressure rises faster than the control valve can open.

This simulation proves that control of a MBSX is achievable and allows the development of a fully automated MBSX system to be developed (Chapter 4). This can be used in Zr and Hf SX studies to obtain improved understanding of MBSX process kinetics. The control of flow rate and pressure exceeds the performance of the manual system used previously, while allowing more precise and repeatable studies to be done.

3.5. References

1. Hallstadius, L., S. Johnson, and E. Lahoda, *Cladding for high performance fuel.* Progress in Nuclear Energy, 2012. **57**(0): p. 71-76.

2. Smolik, M., A. Jakóbik-Kolon, and M. Porański, *Separation of zirconium and hafnium using Diphonix® chelating ion-exchange resin.* Hydrometallurgy, 2009. **95**(3–4): p. 350-353.

3. van der Westhuizen, D.J., *Separation of Zirconium and Hafnium via Solvent Extraction*, in *Chemistry*. 2010, North-West University Potchefstroom. p. 141.

4. Banda, R., S.H. Min, and M.S. Lee, *Selective extraction of Hf(IV) over Zr(IV) from aqueous H2SO4 solutions by solvent extraction with acidic organophosphorous based extractants.* Journal of Chemical Technology & Biotechnology, 2014. **89**(11): p. 1712-1719.

5. Taghizadeh, M., R. Ghasemzadeh, S.N. Ashrafizadeh, K. Saberyan, and M.G. Maragheh, *Determination of optimum process conditions for the extraction and separation of zirconium and hafnium by solvent extraction.* Hydrometallurgy, 2008. **90**(2–4): p. 115-120.

6. van der Westhuizen, D.J., G. Lachmann, and H.M. Krieg, *Method for the selective separation and recovery of metal solutes from solution*. 2012.

7. Kosaraju, P.B. and K.K. Sirkar, *Novel solvent-resistant hydrophilic hollow fiber membranes for efficient membrane solvent back extraction.* Journal of Membrane Science, 2007. **288**(1–2): p. 41 - 50.

8. Rout, P.C. and K. Sarangi, *A comparative study on extraction of Mo(VI) using both solvent extraction and hollow fiber membrane technique.* Hydrometallurgy, 2013. **133**(0): p. 149-155.

9. Kertész, R. and Š. Schlosser, *Design and simulation of two phase hollow fiber contactors for simultaneous membrane based solvent extraction and stripping of organic acids and bases.* Separation and Purification Technology, 2005. **41**(3): p. 275-287.

10. Kertész, R., M. Šimo, and Š. Schlosser, *Membrane-based solvent extraction and stripping of phenylalanine in HF contactors.* Journal of Membrane Science, 2005. **257**(1–2): p. 37-47.

11. Shen, S.F., K.H. Smith, S. Cook, S.E. Kentish, J.M. Perera, T. Bowser, and G.W. Stevens, *Phenol recovery with tributyl phosphate in a hollow fiber membrane contactor: Experimental and model analysis.* Separation and Purification Technology, 2009. **69**(1): p. 48-56.

12. Gabelman, A. and S.-T. Hwang, *Hollow fiber membrane contactors.* Journal of Membrane Science, 1999. **159**(1–2): p. 61-106.

13. Wagner, C., S. Armenta, and B. Lendl, *Developing automated analytical methods for scientific environments using LabVIEW.* Talanta, 2010. **80**(3): p. 1081-1087.

14. Svrcek, W.Y., D.P. Mahoney, and B.R. Young, *A real-time approach to process control*. 2006: Wiley.

15. Atkins, P.W., V. Walters, and J. De Paula, *Physical Chemistry*. 2006: Macmillan Higher Education.

CHAPTER 4: CONSTRUCTION AND AUTOMATION OF AN MBSX

4.1. Introduction

While the growing interest in research done using hollow fibre membranes for metal ion extraction has resulted in an increasing number of publications, considerable work is still required for it to be adopted in the hydrometallurgical industry [1]. MBSX has the potential to become a commonly used technique in the separation or purification of a wide variety of materials ranging from transition and heavy to rare earth and precious metals [2-5]. In MBSX, the membrane primarily acts as a physical barrier between the two phases, making the MBSX system non-dispersive, thereby solving the problems encountered by dispersive solvent contactors (e.g. mixer-settlers) such as emulsions, flooding and foaming [6]. Unlike other membrane separation techniques such as reverse osmosis, which are pressure driven, the MBSX of metals is a concentration driven mechanism, where the membrane only acts as a physical barrier between the aqueous and the organic layers. Accordingly, the membrane does not play a role in the extraction itself [7].

Although the extraction during MBSX is not pressure driven, the control of pressure and flow through the membrane module, which can be classified as the main control parameters, are vital for the controlled and repeatable use of MBSX. Incorrect pressures can lead to aqueous phase breakthrough, contaminating the organic phase and leading to less reliable extraction studies [6]. The control of flow rate through the membrane is equally important as pressure and flow rate are inherently coupled in a closed system such as a membrane contactor.

While various small scale membrane-based experimental setups have been previously automated to increase control and repeatability [8-10], for example the automation of an ultrafiltration experimental setup as described by Curcio et al. [11]. It is apparent from literature, when it comes to MBSX, that most studies not only used similar experimental setups, but, in all cases, used analogue instrumentation [12-17]. This manual setup typically consists of a commercially available hollow fibre membrane, through which the liquids are pumped using either peristaltic or gear drive pumps, while the monitoring of the pressure and flow rate is done using analogue pressure gauges and flow meters, respectively. However, a manual MBSX setup lacks not only precision control elements, but also the possibility of electronic data recording. It is clear that a lack of control in an experimental setup increases the margin of error. Apart from the advantages mentioned above, automation could take MBSX technology a step closer to the industrial application of this technology [18].

Several types of automation hardware and software are commercially available, including programmable logic controllers (PLC) [19]. As discussed in Chapter 2, NI LabVIEW™ is a common system used for laboratory setup automation [20-23] as it is a simple, yet powerful, graphically based programming language that works on flow chart principle, which is specifically

suitable for laboratory automation as it is able to communicate with a wide variety of devices that can generate or accept a signal [24].

While the aim in Chapter 3 was to simulate the control elements of an automated system, it is the aim of this chapter is to design and construct an AMBSX unit that is both flow and pressure controlled and has data logging capabilities. Once constructed, the AMBSX system will be tested for flow rate and pressure stability and extraction repeatability. The AMBSX repeatability will be tested on an Zr and Hf extraction procedure that has been optimised using batch SX [25].

4.2. Method

In this section a general description of the design and development of an AMBSX is given, while the actual diagrams, materials chosen and results are presented in Section 4.3.

4.2.1 Process flow diagram

A PFD for the AMBSX unit was based on the manual experimental setup flow diagram used previously in our group [26]. The general manual system, as shown in Chapter 2 (Figure 2-3), used two positive displacement gear drive pumps to pump the liquids from the feed tanks through the membrane contactor before recirculating back into the feed tanks. Since the flow rate had been controlled using two manual control needle valves, the MBSX system required calibration every time the flow rate was changed as no in-line flow meters were used. The pressure, on the other hand, was measured using four in-line analogue pressure gauges situated at the inlets and outlets of the membrane's shell and lumen connection ports. Furthermore, no temperature monitoring was done with the manual system, nor did it include a sampling system (sampling was done from the feed tanks).

For the AMBSX system the metering equipment was replaced with digital output gauges, including electronic pressure gauges, in-line electronic turbine flow meters and resistance temperature detectors (RTD). The pumps selected for the AMBSX were gear drive pumps, similar to the pumps used in the manual system; however, for the electronic control and data logging, the new gear drive pumps have 4-20 mA electronic input connections in the form of RS232 ports, allowing the pumps to be controlled by a central controller. Three-way electronic solenoid valves were used both as sampling elements and to control the direction of flow. Additionally, an in-line membrane filter was introduced into the system as a precautionary measure to protect the equipment and hollow fibre membrane from any debris or precipitates entering the feed streams. The PFD also included cleaning solution feed tanks and chemical waste containers.

All equipment materials were selected to withstand the high acid concentrations and non-polar organic solvents that are commonly used in MBSX research. This implies that the materials should be able to withstand acids of up to 9 mol/L, while being resistant to strong organic solvents, such as cyclohexane, heptane and kerosene. The materials used in the wetted parts of the process (pipes, fittings, pump heads, filters, valves and membrane) include PTFE, PP, PFA and PVDF. Polypropylene piping with a ¼" outer diameter and the required push-to-connect fittings were used. The AMBSX was designed for a standard co-current flow direction, but flow direction switching across the membrane was included for more flexibility, which was achieved with four three-way valves that reroute the lumen inlet and outlet ports, changing the membrane setup from co-current to cross-current.

The control elements of the AMBSX system, namely the aqueous and organic flow rates and pressure were controlled by the pump gear rotation speed and by electronic pressure control valves. This implies that, after obtaining a signal from the turbine flow meter, the central controller adjusts the pump's rotation speed to control the set flow rate. Similarly, the pressure was controlled by means of electronic control needle valves that adjust the valve opening according to the pressure obtained from the inlet pressure gauges. As discussed and simulated in Chapter 3, the control elements (flow rate and pressure) will be PID controlled using the Cohen-Coon and trial-error fine tuning discussed in Chapter 3.

For the control of the AMBSX, National Instruments'™ equipment was obtained to facilitate the communication with LABVIEW™. A CompaqRio 9022 controller fitted with an eight slot cRIO-9112 chassis was chosen as the central controller for the AMBSX system. The CompaqRio 9022 has a 533MHz processor and FPGA for high speed data monitoring. As the controller uses modular input/output modules, the system was adapted to the AMBSX system requirements by including analogue input and output modules that use a 4-20 mA signal to detect and control the electronic pumps, valves and gauges used in the AMBSX system. The controller was interfaced with a host computer via a 100 Mbit/s Ethernet connection.

As mentioned previously, the gear drive pumps and electronic pressure control valves used a 4-20 mA analogue input signal to control the speed of rotation or percentage opening of the valve. A NI 9265 module was fitted to the chassis to connect the pumps and control valves to the central controller. The NI 9265 is a four channel, 16 bit module that connects to the equipment using two wire connector terminals, namely AO, which connects to the signal wire of the device, and a common terminal, which connects to the ground wire. The NI 9265 module requires an additional power supply line and was connected to a 24V DC power supply via the V_{sup} and Power Supply ground terminals. The RTD temperature probes were connected to the CompaqRio via the four channel 24 bit NI 9217 module. This is a dedicated analogue input RTD module that supports

three wire RTD's using terminals RTD+ for the positive wire of the device and RTD- and COM for the negative leads.

The four pressure gauges used were connected to the CompaqRio via an NI 9208 analogue input module. This 16 channel 24 bit module, which measures 4-20 mA signals produced by the pressure gauges, was connected via a two-wire system where the AI terminal was connected to the signal wire and the common terminal to the ground wire of the pressure gauge. This module also requires additional power and connects the positive lead of a 24V DC power supply to the V_{sup} and the negative lead to a COM terminal. Since the turbine flow meters produce a square wave pulse signal, a high speed analogue input module is required. For this purpose the NI 9221, which is an eight channel 12 bit module, was selected, as it has a high sampling rate (800 000 samples per second).

4.2.2 Flow rate calibration

The in-line turbine flow sensors operate by detecting the rotation of the turbine blade caused by the fluid moving through the turbine. The edge of the turbine blade is coated with an infrared reflecting material and, using an infrared sensor, a square wave pulse is produced as the blade passes the sensor. The square wave pulse can be represented as a binary system, with 0 volts as off (or 0) and 24 volts as on (or 1). The flow rate is calculated using the number of pulses produced per second. The flow meters were calibrated by the manufacturer at a specified number of pulses per litre for water at 25°C. As the central controller would have to detect the square wave signal, as displayed in Figure 4-1, at a high number of pulses per second, an FPGA chip was needed to reduce any latency of the pulse detection. The FPGA was used by coding a signal detection program, which scans the input device (NI 9221) for a change in the input voltage from 0 volts to 24 volts. A rise in voltage indicates a single pulse causing a pulse counter to incrementally increase. The number of pulses detected per second is given as the flow rate in L/s which was then converted to ml/min.

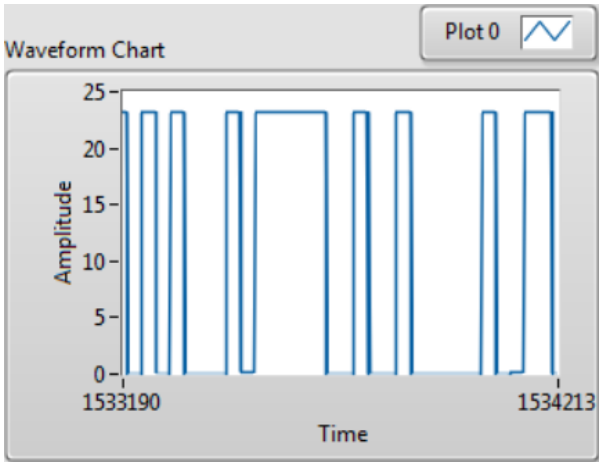

Figure 4-1: Square wave output of the turbine flow meters

As the flow sensors come into direct contact with the solutions, viscosity of the fluid can influence the accuracy of the flow rate measured. Thus, the flow meters require calibration for different liquids, which was done by adjusting the calibration variable K-factor, which is represented in pulses per litre. Each flow sensor is issued with a calibration K-factor value for water, which must be calibrated for other liquids to ensure accuracy.

For this purpose, LabVIEW™ was again used to program an automated calibration procedure. For calibration, the flow rate of the AMBSX system was allowed to reach a set value, while the pressure control values were set to 100% open to minimize backpressure effects. Once equilibrium has been reached, a calibration button was pressed, opening a relevant sample valve (aqueous or organic) for 30 seconds, depositing a sample with a known volume in a sample container. This was repeated for the entire range of flow rates. From the obtained data, a calibration graph was constructed by plotting the recorded volume on the y-axis and the measured volume on the x-axis. The slope (h) obtained from the graph was subsequently used in the following equations to determine the k value:

$$hk = \frac{\Delta y}{\Delta x} \tag{1}$$

$$\therefore k = \frac{1}{h} \tag{2}$$

The obtained k value was multiplied by the initial K-factor to obtain a corrected K-factor value, which was used to correct the control program.

Once the flow meters had been calibrated, a graph was constructed representing the natural back pressure of the system. This was attained by running the AMBSX system using deionised water as the aqueous feed and cyclohexane as the organic feed. The inlet and outlet pressures of the

shell and lumen sides at different flow rates were recorded at flow rates of 100, 125, 150, 200, 300, 400, 500, 600, 700 and 800 ml/min. The natural backpressure of the system was used to determine the minimum usable operating pressures of both the aqueous and organic streams.

4.2.3 Control and PID optimisation

To control the aqueous and organic flow rate and pressure of the AMBSX, proportional, integral and derivative (PID) control algorithms were used, which were optimised using Cohen-Coon and fine-tuned using a trial and error approach as described in Chapter 3. LabVIEW's™ built-in PID subprogram (named "PID.vi") was used to program the PID algorithm, an example of which is presented in Figure 4-2. The built-in PID function requires three main inputs to function, namely PID gains, process variable and set point, while the other inputs such as output range are available, but not required. The PID gains sets the three PID variable controls: i) the proportional gain (K_c), ii) the integral time in minutes (T_i) and iii) the derivative time in minutes (T_d). The process variable input of the PID program, which in this case was either current flow rate or pressure, was controlled. The set point input was the user-defined value to which the PID adjusted the process variable. Once all the inputs were entered, the PID.vi output a value in percentage, which was used to control the pump rotation speed or the pressure control valve position. The PID optimisation was firstly done for the flow rate with the pressure control valves at 100% open. Subsequently, the PID control for pressure was optimised. During calibration, the aqueous stream was always calibrated first, followed by the organic stream, to ensure that the aqueous pressure remained higher than the organic pressure to prevent breakthrough of solvent through the hydrophobic membrane. The results obtained during the PID optimisation are discussed for both flow rate and pressure in Sections 4.2.5.1 and 4.2.5.2 respectively.

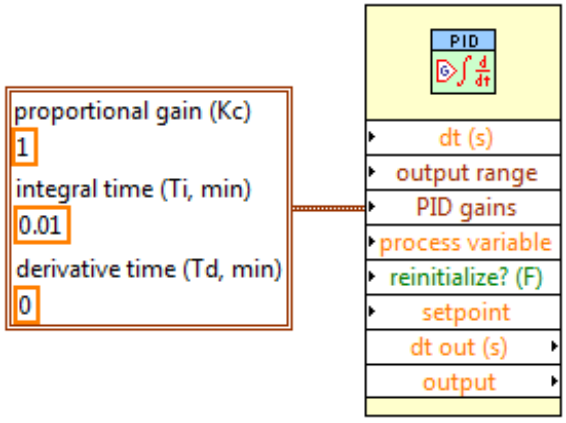

Figure 4-2: PID algorithm function as seen in LabVIEW™

4.2.3.1 Flow rate control

After calibration of the flow rate, the control PID optimisation for flow rate was done for both aqueous and organic streams by firstly filling the aqueous and organic feed tanks with deionised water and cyclohexane, respectively. The PID gains variables, namely K_c, T_i and T_d, were adjusted using values obtained from the simulation results (Chapter 3) to ensure a stable flow rate with no oscillation. Once both pumps had been started and a steady state flow rate of 100 ml/min for the aqueous stream had been obtained, a change in the set point from 100 ml/min to 500 ml/min was applied. This resulting disturbance was then plotted on a graph and the Cohen-Coon method applied as discussed previously. Once optimisation had been attained, this procedure was repeated for the organic stream.

4.2.3.2 Pressure control

After the PID optimisation of flow rate had been obtained, a similar procedure was followed for the pressure calibration. The same aqueous and organic solutions that had been used in the flow rate optimisation were used in the pressure optimisation. The flow rate was set at 100 ml/min, resulting in a steady state pressure of 30 kPa. The PID gains values (K_c, T_i and T_d) that were obtained in the simulation results for pressure (Chapter 3) were used to help adjust the pressure PID gains values to achieve steady state. The set point was then changed from 30 kPa to 60 kPa and the resulting graphs used to apply the Cohen-Coon method. This method was repeated for the organic pressure control.

4.2.4 Automated sampling

The AMBSX system was programmed with an automated sampling program, which allows the operator to input sampling times into the program before each experiment. To maintain aqueous to organic (a/o) volume ratios, the sampling system was constructed and programmed to remove equal volumes of both aqueous and organic solutions when sampling. A timer was programmed to begin once the flow rate and pressures of both aqueous and organic sides had achieved the required set points. When reaching a sampling time, the program opened both aqueous and organic sampling valves. The valves remained open until 10 ml of sample had been deposited in a sample holder, which had been determined using the flow rates. Sample containers were replaced manually. Subsequently, the metal concentrations in the aqueous samples were analysed using an inductively coupled plasma optical emission spectrometer (ICP-OES), as described in Chapter 4.2.7 while the organic sample was disposed in a liquid waste storage container.

4.2.5 Internal volume and breakthrough pressure

The AMBSX total internal volumes of both the aqueous and organic sides of the system were determined by firstly draining and drying the system with nitrogen gas for 20 minutes. The aqueous and organic feed tanks were then filled with 1L of water and cyclohexane, respectively. The aqueous pump was started and set to 100 ml/min. As soon as solution exited the system, the pumps were stopped and the volume of the remaining solution in the feed tanks determined, from which the internal volume of the aqueous phase was determined. Subsequently, the aqueous side was set to recirculate so that the volume of the organic side could be determined in a similar manner.

The breakthrough pressure (as described by Gabelman and Hwang [6]) of the system was determined experimentally by firstly setting the flow rates of the system at 400 ml/min for both aqueous (deionised water) and organic (cyclohexane) streams, while setting the aqueous and organic pressure at 50 kPa and 40 kPa, respectively. The aqueous pressure was then systematically increased until breakthrough (the aqueous solution appeared in the organic feed tank) was observed.

4.2.6 Operational procedure

The AMBSX experimental start-up, run-time and shutdown procedures are displayed in Figure 4-3. Firstly, a safety check is done to ensure pipes, fittings and equipment are securely mounted and that there are no visible signs of damage. The equipment is powered on and checked for any faults. The feed tanks are filled while the cleaning solution's tank levels checked. Once the pre-start checks have been completed, the user must input the experimental parameters including the required flow rates, pressures and sampling times. Subsequently, the aqueous side is started. Once the system has filled and the flow rate has been stabilised, the pressure control switch is activated to ensure that when the organic phase is introduced, the aqueous pressure remains higher than the organic pressure to avoid breakthrough. Finally, the organic pump is started and the organic pressure control activated before starting the experiment recording and timer.

While sampling will occur automatically at the predefined times, the operator must remember to replace the sample holder after every sample taken. After completing the experiment, the shutdown procedure is initiated by stopping the organic pump and pressure control, followed by the aqueous pump and pressure control. The aqueous side cleaning procedure entails flushing the aqueous side with deionized water while the organic side is flushed using clean solvent. Subsequently, the system is dried by purging both sides of the AMBSX with nitrogen gas. The data containing the aqueous and organics flow rates, pressures and temperatures of the

experiment are then exported and saved. During the final step, the equipment is powered off, followed by a final inspection of the pipes, fittings and equipment.

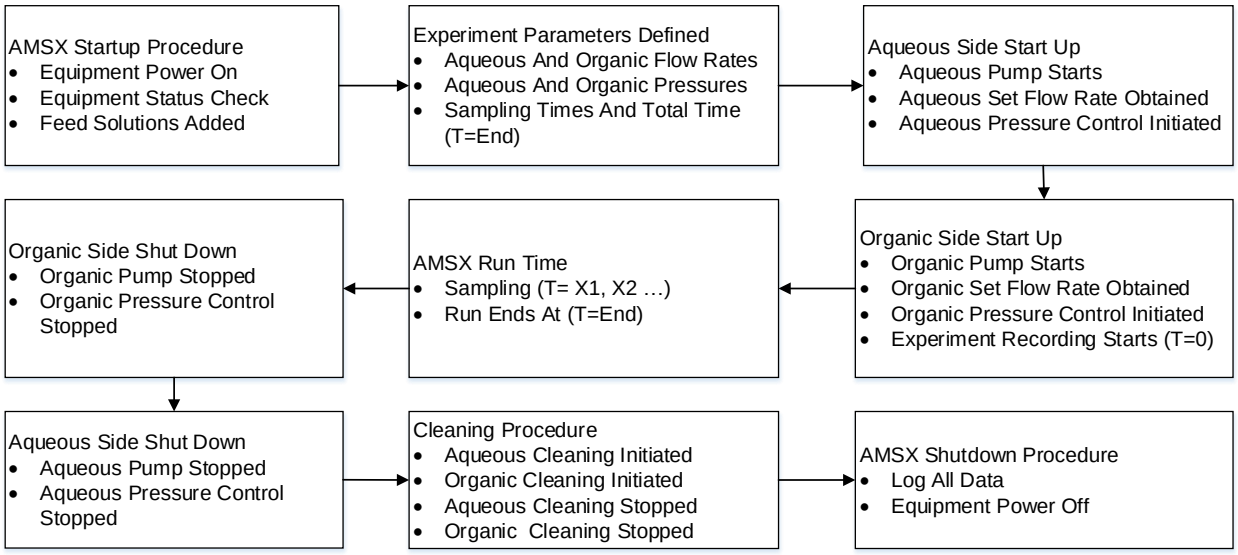

Figure 4-3: Flow diagram of the AMBSX start-up, run-time and shutdown procedure

4.2.7 Case Study

The novel designed and constructed AMBSX system was tested using the conditions determined from a batch extraction process developed by De Beer et al. [25]. According to the batch process results, optimum extraction and selectivity were attained when using an H_2SO_4 containing aqueous phase and a Cyanex 301® (bis(2,4,4-trimethylpentyl)dithiophosphinic acid) containing cyclohexane organic phase. Both metal salts, $ZrCl_4$ and $HfCl_4$, were obtained from Sigma-Aldrich and were used without further purification. Sulphuric acid (98% H_2SO_4), cyclohexane and 1-octanol were obtained from Merck and used without further purification. The deionized water used throughout the entire study, with a >18 MΩ/cm resistivity, was prepared using a Millipore Milli-Q purification system. The extractant Cyanex 301®, was obtained from Cytec Canada Inc. The aqueous phase was prepared by dissolving 1.0 g/L $ZrCl_4$ and 0.03 g/L $HfCl_4$ in 1L of water containing 0.5 M H_2SO_4. The organic phase was prepared by dissolving the Cyanex 301® in a solution of cyclohexane containing 5 % (v/v) 1-octanol. The extractant concentration (47.752 g/L) was set at an extractant to metal ratio of 30:1. Both solutions were aged at 25°C for 24 hours, before being contacted using the AMBSX setup.

The AMBSX aqueous flow rate was calibrated for both the 0.5M H_2SO_4 and cyclohexane solution as described in Chapter 4.2.2. The K-factors for the aqueous and organic flow rate sensors were adjusted to 91464 and 98757 pulses per liter, respectively. The aqueous flow rate was set to 450

ml/min at 100 kPa while the organic flow rate was set to 350 ml/min at 70 kPa. Total contact time was 120min with 10 ml samples of each phase taken at 0, 1, 3, 5, 7, 10, 15, 20, 25, 30, 40, 50, 60, 70, 80, 90 and 120 minutes. This extraction was repeated five times to determine the stability (flow rate and pressure) and repeatability of the AMBSX. While the temperature was not controlled, a temperature profile for the aqueous and organic phases over the duration of the experiments was obtained.

The aqueous samples were analysed using an ICP-OES using a Thermo Scientific iCap 6000 series ICP-OES coupled with iTEVA software. Aqueous samples obtained from the AMBSX were analysed as received from the AMBSX. ICP-OES calibration solutions with concentrations of 50, 200 and 400 mg/L for Zr and 10, 30 and 50 mg/L for Hf were prepared by diluting ICP-OES Zr and Hf standard solutions (1 g/L), obtained from De Bruyn Spectroscopic Solutions, and using 0.5M H_2SO_4 stock solution. The ICP-OES was calibrated before any batch of samples was analysed, a minimum correlation of value of R = 0.9999 was used ensure the accuracy of calibration. A Quality control solution of 200 and 30 mg/L Zr and Hf was prepared from the verified reference standards obtained from De Bruyn Spectroscopic Solutions. The quality control solution is analysed after five sample intervals to determine if the ICP-OES needs to be recalibrated. If the quality control measured values are larger than 5% of the set value of 200 mg/L Zr and 30 mg/L Hf, the ICP-OES was set to recalibrate and re-run the last 5 samples. The relative standard deviation as investigated by Branken [27], showed a maximum RSD% = 0.529, and the emission lines, which were selected to minimise interference, for Zr and Hf were 274.2 nm and 339.9 nm, respectively.

4.3. Results and discussion

4.3.1 Process flow diagram

The AMBSX PFD is shown in Figure 4-4 with a description of all the components listed in Table 4-1. The aqueous side of the PFD consists of an aqueous feed tank T-A1 containing a RTD probe RDT-A1 (type K probe) to measure and log the feed solution temperature. The feed tank is connected to a three-way electronic solenoid valve that will route the stream either from T-A1 or T-A2 (aqueous cleaning solution tank) to the gear drive pump. The pump outlet leads to the PTFE membrane in-line filter F-A1 followed by the PFA in-line turbine flow sensor FM-A1and the inlet pressure gauge manifold PI-A1. The aqueous stream is connected to the shell side inlet port of the membrane. Exiting the membrane, the stream passes the outlet pressure gauge PI-A2, the electronic pressure control valve EPCV-A1, through the three-way valve V3-A2, which will route the stream to either the waste collection tank T-A3 or return it to the feed tank T-A1. The organic side is similar in configuration to the aqueous side; however, four additional valves are required

for flow direction change (V3-O2, V3-O3, V3-O4 and V3-O5), which by default was set in a co-current flow direction. The flow rate range of both aqueous and organic sides was limited to 100-850 ml/min. The maximum internal pressure of the system was limited to 200 kPa by the electronic solenoid three way valves failing after a pressure of 200 kPa.

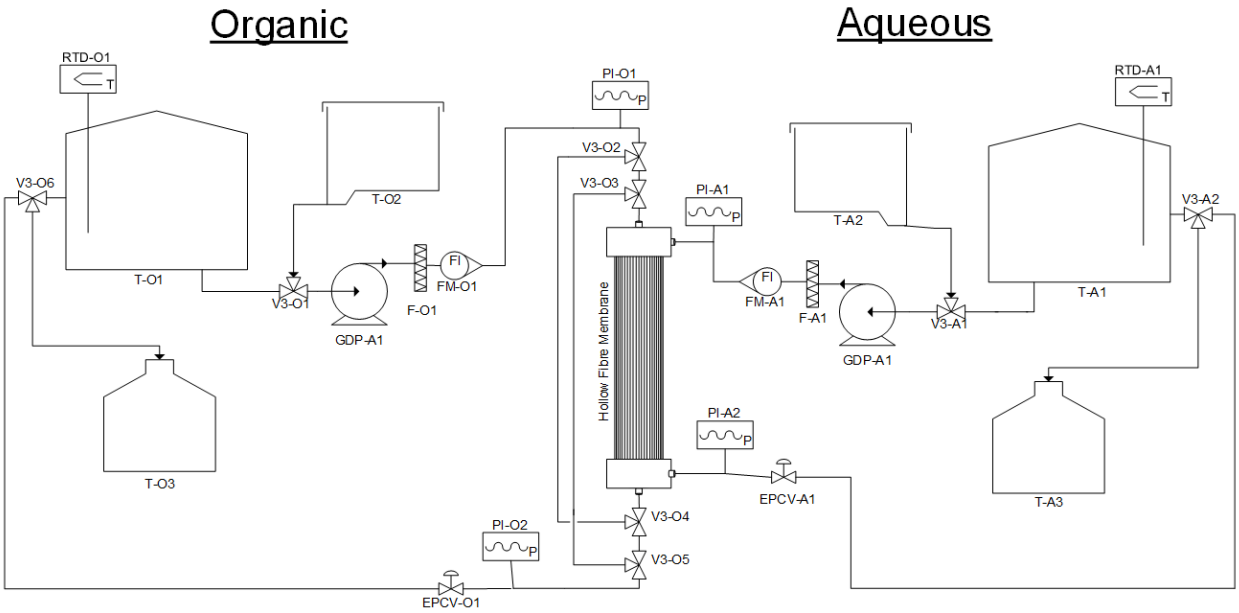

Figure 4-4: PFD of the AMBSX system

Table 4-1: AMBSX equipment list

Label	*Description*	*Connection*	*Material*	*Manufacturer*
EPCV-A1	Electronic Pressure Control Valve	1/4" NPT	PTFE Coated	Hanbay Inc
EPCV-O2	Electronic Pressure Control Valve	1/4" NPT	PTFE Coated	Hanbay Inc
FM-A1	PFA Turbine Flow Sensor	1/4" Barbed	PFA	Equflow® Sensors
FM-O1	PFA Turbine Flow Sensor	1/4" Barbed	PFA	Equflow® Sensors
GDP-A1	Gear Pump Drive	1/8" NPT	PTFE	Cole-Parmer®
GDP-O1	Gear Pump Drive	1/8" NPT	PTFE	Cole-Parmer®
F-A1	In-Line PFA Filter/PTFE Membrane	1/4" Barbed	PFA / PTFE	Cole-Parmer®
F-O1	In-Line PFA Filter/PTFE Membrane	1/4" Barbed	PFA / PTFE	Cole-Parmer®
PI-A1	BDS-Pressure Gauge TRX	G 1 1/2"	PTFE / Ceramic	BD Sensors®
PI-A2	BDS-Pressure Gauge TRX	G 1 1/2"	PTFE / Ceramic	BD Sensors®
PI-O1	BDS-Pressure Gauge TRX	G 1 1/2"	PTFE / Ceramic	BD Sensors®
PI-O2	BDS-Pressure Gauge TRX	G 1 1/2"	PTFE / Ceramic	BD Sensors®
RTD-A1	RTD PTFE coated probe 100 ohm	-	PTFE Coated	Digi-sense
RTD-O1	RTD PTFE coated probe 100 ohm	-	PTFE Coated	Digi-sense
T-A1	Aqueous Feed Solution Tank	-	Glass	-
T-A2	Aqueous Cleaning Solution Tank	-	Polypropylene	-
T-A3	Aqueous Waste Tank	-	Polypropylene	-
T-O1	Organic Feed Solution Tank	-	Glass	-
T-O2	Organic Cleaning Solution Tank	-	Polypropylene	-
T-O3	Organic Waste Tank	-	Polypropylene	-
V3-A1	3-Way Direct Lift Solenoid Valve	1/8" NPT	PTFE	Valcor®
V3-A2	3-Way Direct Lift Solenoid Valve	1/8" NPT	PTFE	Valcor®
V3-A3	3-Way Direct Lift Solenoid Valve	1/8" NPT	PTFE	Valcor®
V3-A4	3-Way Direct Lift Solenoid Valve	1/8" NPT	PTFE	Valcor®
V3-A5	3-Way Direct Lift Solenoid Valve	1/8" NPT	PTFE	Valcor®

V3-A6	3-Way Direct Lift Solenoid Valve	1/8" NPT	PTFE	Valcor®
V3-O1	3-Way Direct Lift Solenoid Valve	1/8" NPT	PTFE	Valcor®
V3-O2	3-Way Direct Lift Solenoid Valve	1/8" NPT	PTFE	Valcor®

4.3.2 Flow rate calibration

As discussed in Section 4.2.2, the square wave output of the turbine flow meters requires a pulse detection program to determine the flow rate. Due to the high rate of sampling (up to 1600 pulses per second) the program was coded on the CompaqRio FPGA chip. This enables the pulse detection program to operate independently from the host computer, allowing the detection of the high pulse rate without any latency. The FPGA program, shown in Figure 4-5 a, scans (at 100 kHz) the input device's channel 1 (AI0) for the aqueous and channel 2 (AI1) for the organic flow rate pulses for a rise in voltage. When a rise is detected, the value is incremented to 1. Subsequently, the program waits for the voltage to fall back to 0 volts before another rise can be detected. The total number of pulses detected in 1 sec is sent to the main program that is located on the host computer, where a program (Figure 4-5 b) multiplies the number of pulses detected by the K-factor to give a flow rate in ml/min.

a)

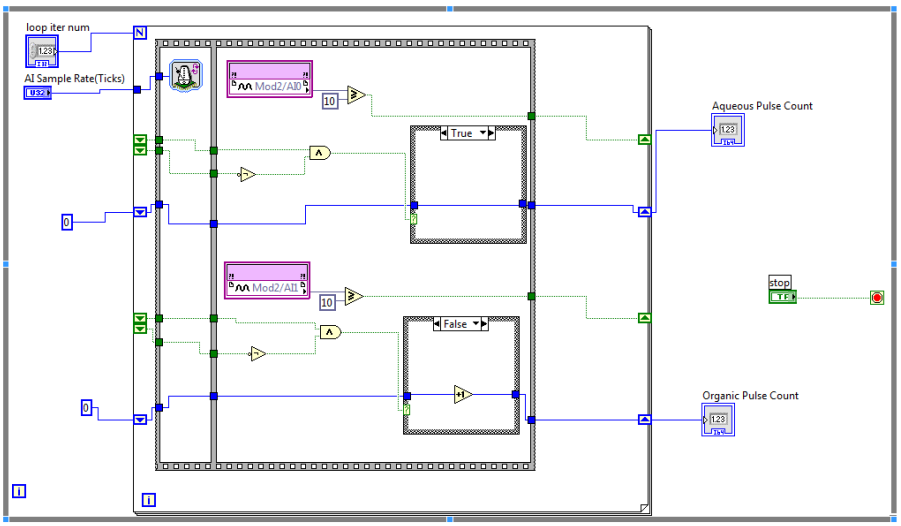

b)

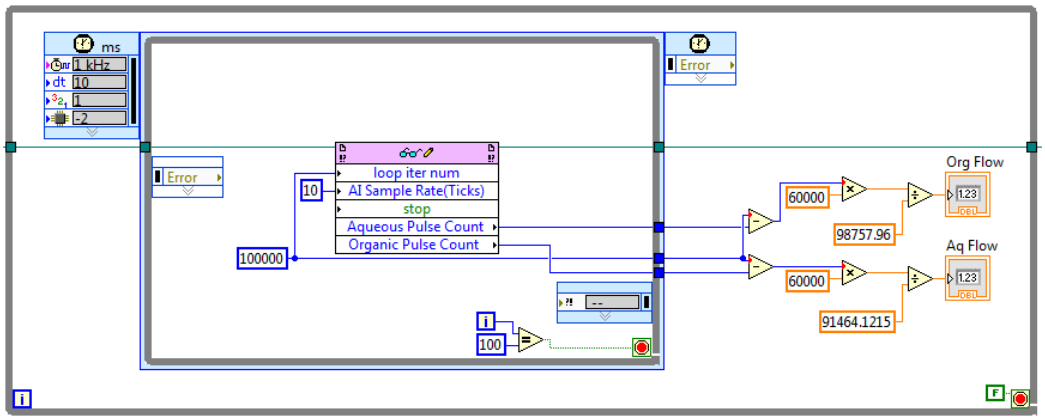

Figure 4-5: a) The FPGA square wave signal detection program code and b) the flow rate calculation program code

In Figure 4-6 the block diagram code that was written for the aqueous calibration program and the corresponding front panel display are presented, while Figure 4-7 and Figure 4-8 show the initial calibration graphs obtained from the aqueous and organic flow meters for water and cyclohexane, respectively. It is clear that for both solvents, a high accuracy (R^2 = 0.9956 and 0,9996 for the aqueous and the organic flow rates, respectively) was attained. The data was used to adjust the K-factor values for water and cyclohexane to 103718 and 91519 pulses/L, respectively (see Section 4.2.2). Keep in mind that the calibration would have to be repeated if different solvents were used.

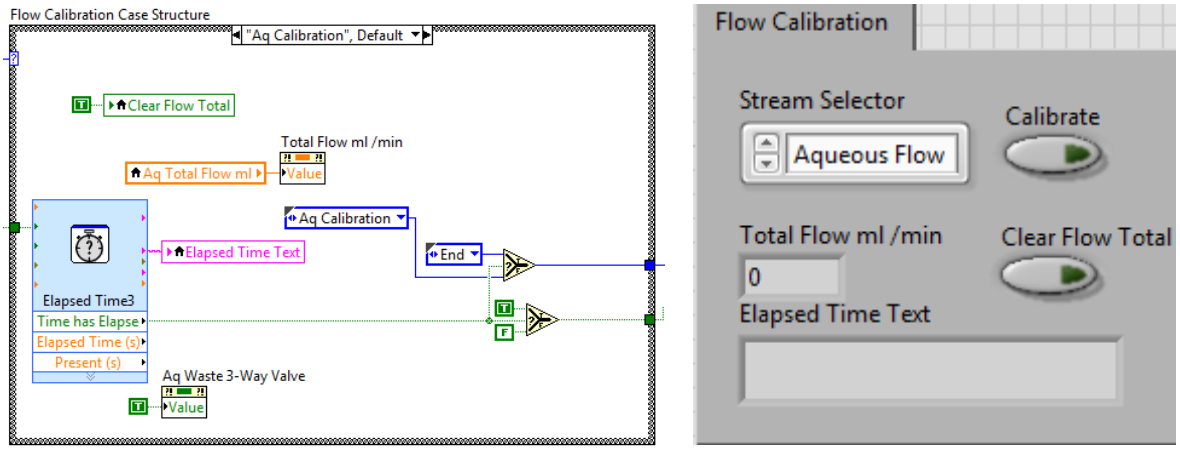

a) b)

Figure 4-6: Flow calibration block diagram a) and front panel b) used for aqueous flow rate

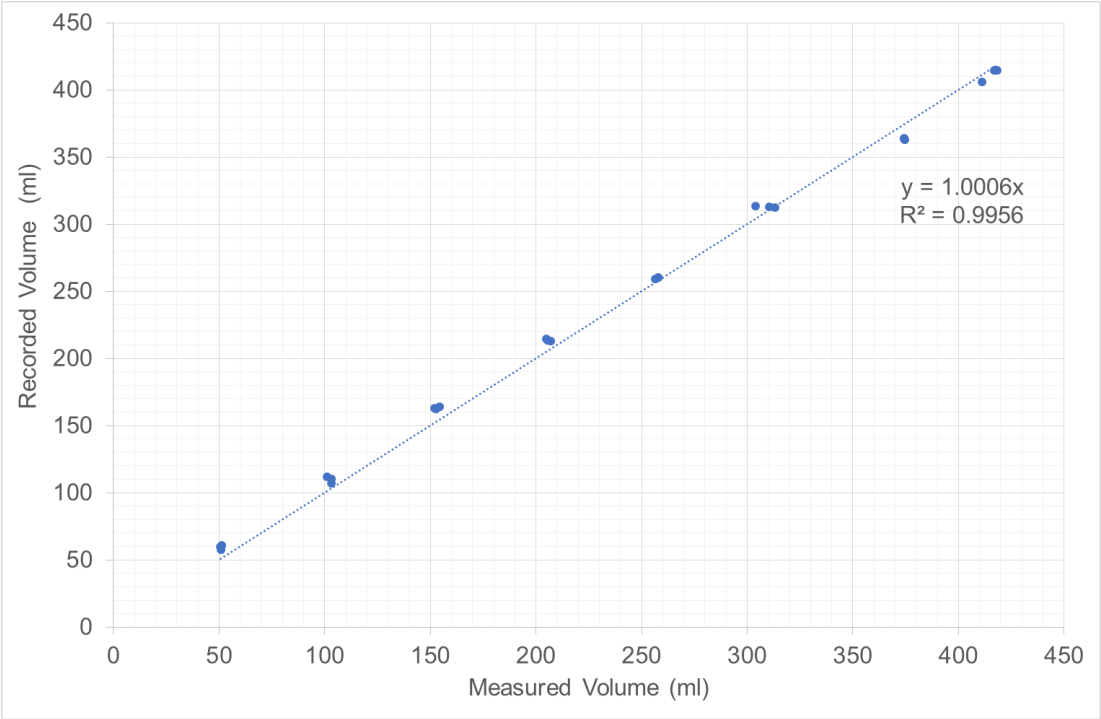

Figure 4-7: Aqueous flow rate calibration graph

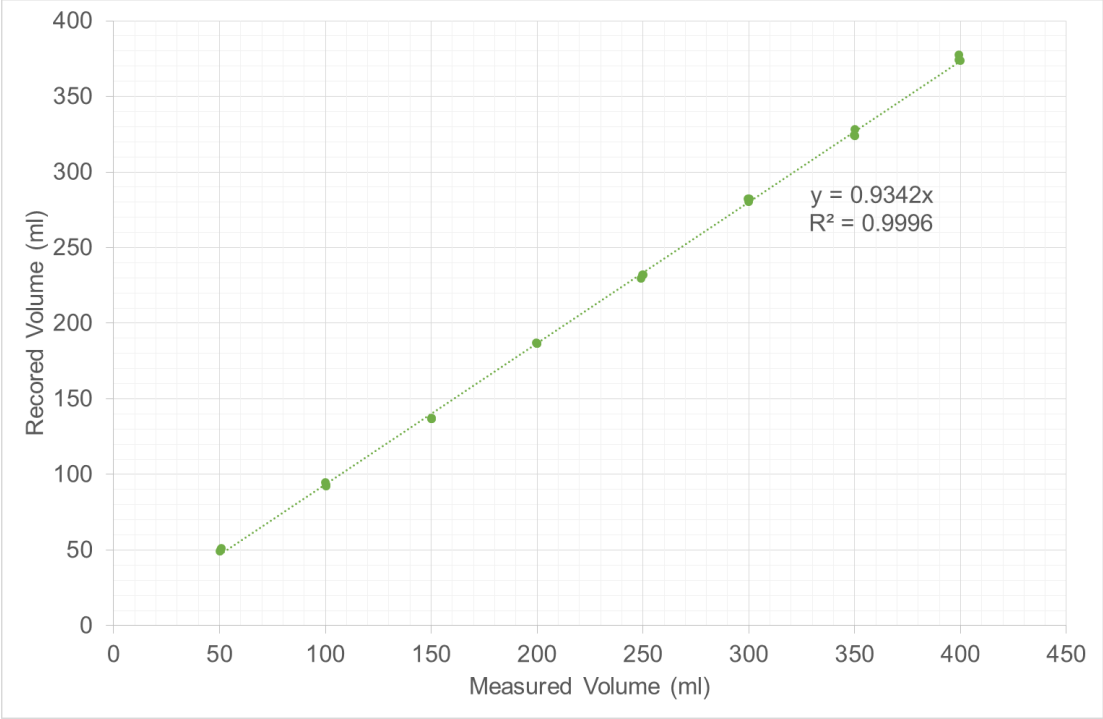

Figure 4-8: Organic flow rate calibration graph

After completing the flow rate calibrations, the AMBSX minimum internal pressure at varying flow rates was determined as displayed in Figure 4-9. As was expected, the pressure increased with increasing flow rates. In addition, the pressure drop over the membrane module, as well as the

difference in the pressure between the aqueous and the organic phase, can be seen. The internal pressures obtained were used to ensure that the minimum pressure during experimental runs was high enough to be controlled by the electronic pressure control valves as a set point below the curve at a certain flow rate could result in an increase in the pressure which might result in phase breakthrough.

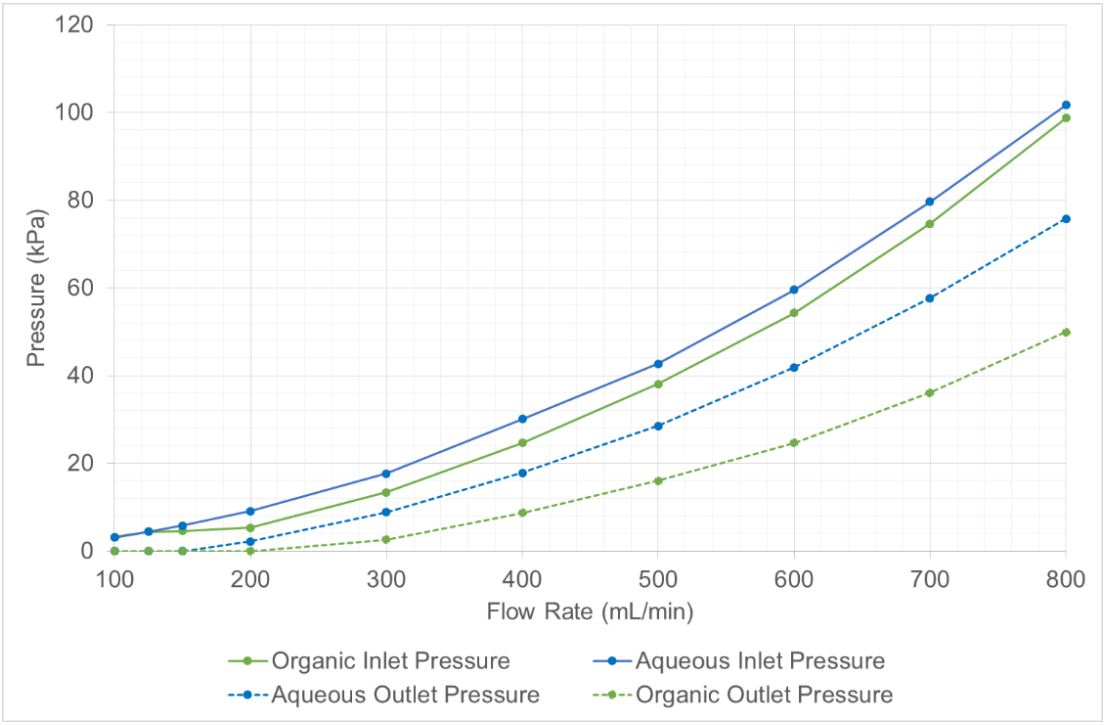

Figure 4-9: AMBSX minimum operating inlet and outlet pressures for aqueous and organic streams using water and cyclohexane solutions

4.3.3 Control and PID optimisation

The aqueous and organic flow rate control and optimisation will be discussed in Chapter 4.3.3.1 and the aqueous and organic pressure control and optimisation in Chapter 4.3.3.2.

4.3.3.1 Flow rate control

In Figure 4-10, the PID control programs of the aqueous and organic flow rates are displayed. The process variable input was obtained from the measured flow rate presented in Section 4.3.2. The set point is read from an input box (front panel), which is set by the operator, while the PID gains variables were optimised using the Cohen-Coon tuning method.

a)

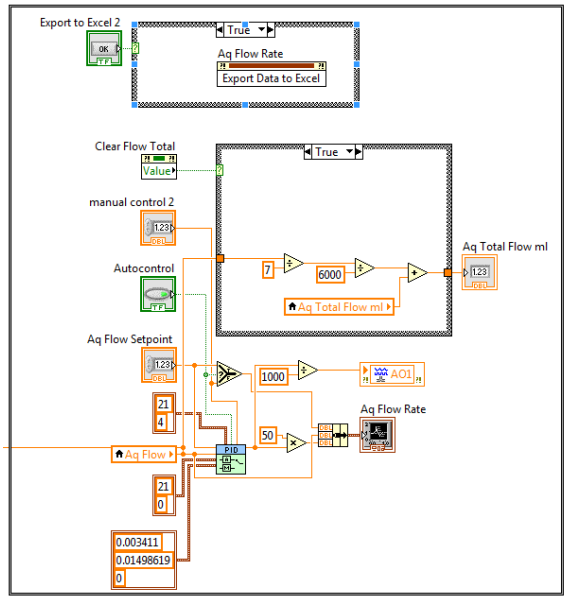

b)

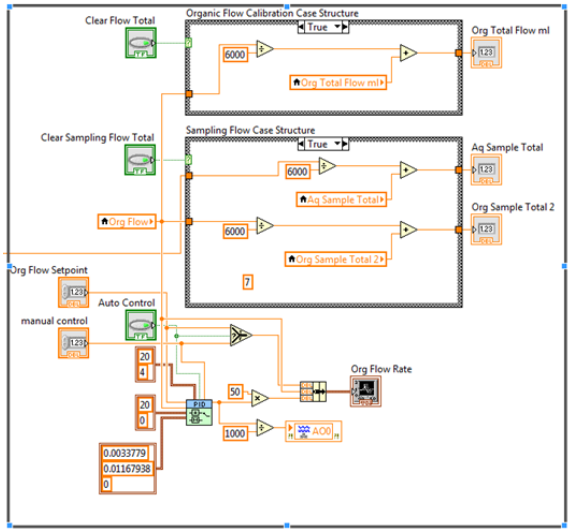

Figure 4-10: Block diagram code of the PID control used for the a) aqueous flow rate and b) organic flow rate

The PID optimisation of the aqueous flow rate is shown in Figure 4-11. Proportional only (P) control is not displayed on the graph as it produced an unstable oscillation, The output signal did not reach a steady state required for the Cohen-Coon method, is characteristic of P-control theory as described by Svrcek et al. [28]. According to the presented results, both the proportional integral (PI) and proportional integral derivative (PID) did stabilise. Although the PI produced a slower rise to the set point than the PID, the PID exceeded the set point and started oscillating after three minutes. Hence the PI control was fine-tuned using the trial-error method by incrementing the P and I values to obtain improved control. It is clear, according to Figure 4-11, that the PI+ fine tuning (2) yielded the optimal results, where the flow rate reached its set point approximately 18 seconds after the change in set point. The final PI values obtained were K_c = 0.0341 and T_i = 0.0149 min.

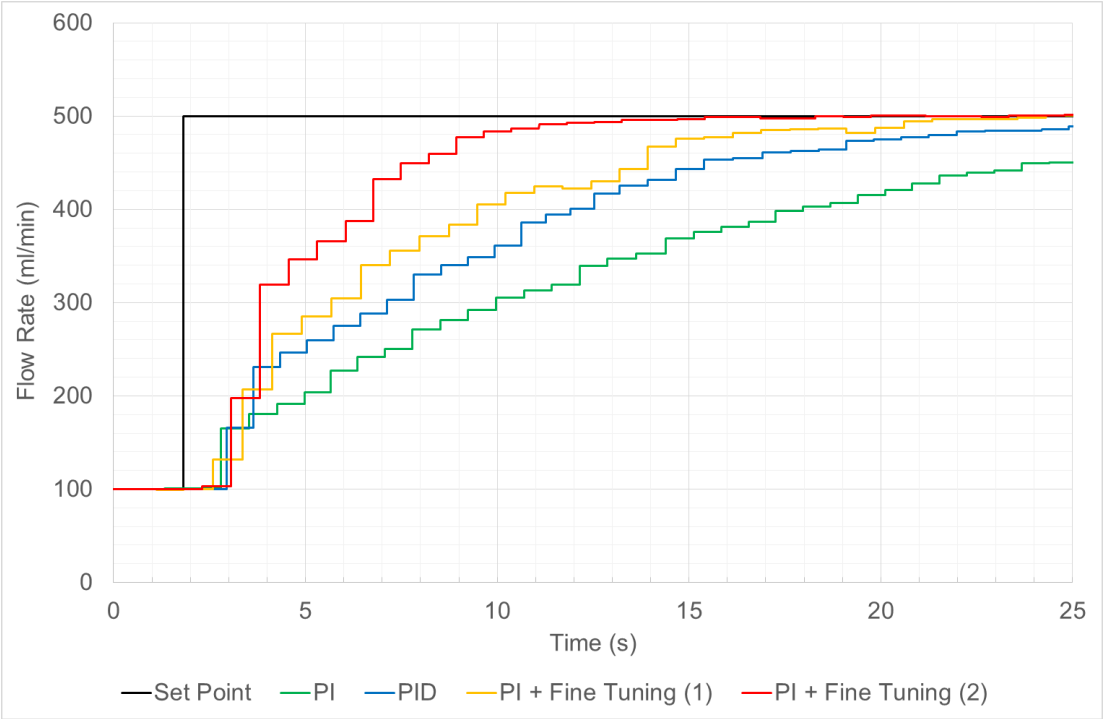

Figure 4-11: Aqueous flow rate PID optimisation using Cohen-Coon and fine tuning methods

The PID optimisation of the organic flow rate is displayed in Figure 4-12. As discussed in the aqueous flow rate optimisation, the P control was again not displayed due to an unstable oscillation. Cohen-Coon was implemented on the PI and PID. Since both PI and PID produced a similar output, PI was chosen for further optimisation using the trial-error method. After optimisation, the PI+ fine tuning (2) gave the best results, where the flow rate reached its set point approximately 16 seconds after a change in set point. The final PI values obtained were K_c = 0.0337 and T_i = 0.0116 min.

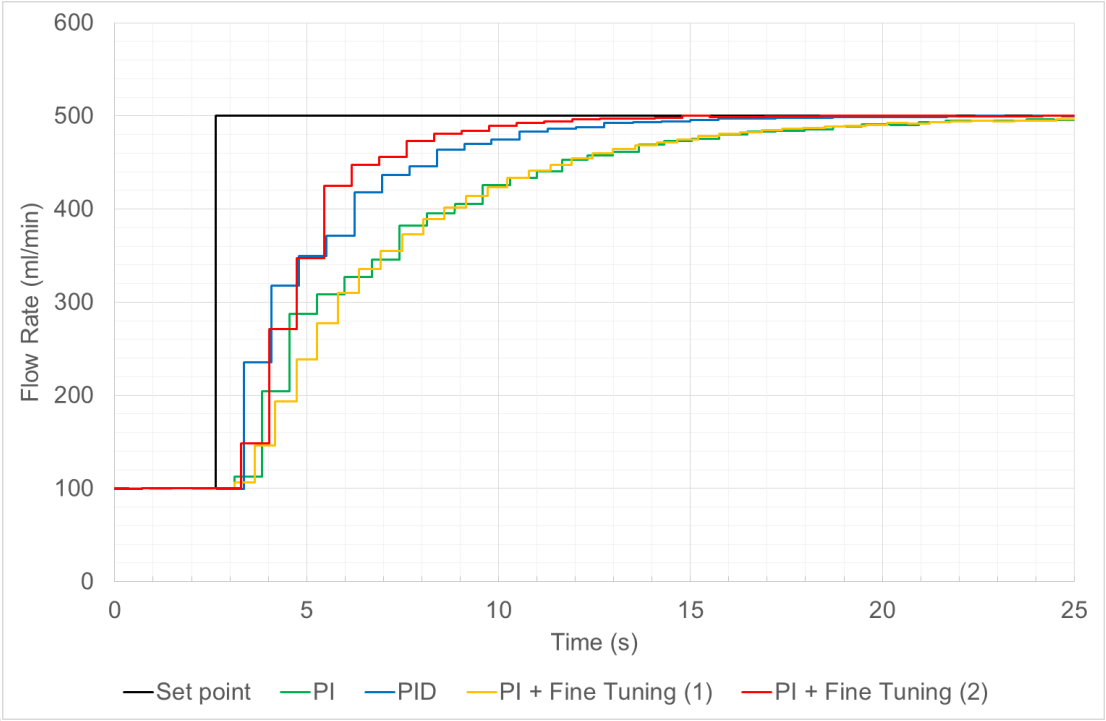

Figure 4-12: Organic flow rate PID optimisation using Cohen-Coon and fine tuning methods

4.3.3.2 Pressure control

The block diagrams of the PID programs that were used for the aqueous and organic pressure control (a and b) are presented in Figure 4-13. While the pressure PID programs had been coded in a similar way to the flow rate programs using the built-in PID function, the pressure was controlled from the value of the inlet pressure gauges of the shell and lumen. The flow rate program uses an electronic pressure control valve as the control element for the pressure by opening or closing the valve orifice. This required that the K_c value had to be given in a negative value. Subsequently, if a higher pressure was needed, the PID reduced the orifice size by closing the valve, while the valve would open to increase the pressure if the K_c had a positive value.

The pressure control was programmed with a slow response time as it was found that if the pressure was adjusted too quickly, the system became unstable as the change in pressure resulted in the pressure control valve being closed too quickly, causing the flow rate to drop, which in turn triggered the pumps to increase the flow rate by increasing the pump rotation speed, leading to a higher pressure. The PID would then try to counter the pressure increase by opening the valve and causing the pressure to drop, which will, however, also cause the flow rate to over shoot the set point, causing the pumps to decrease the flow rate and the pressure control valves to close, repeating the cycle. This was overcome by reducing the pressure control valve's response time so that the flow rate could stabilise before the pressure control has had time to adjust.

a)

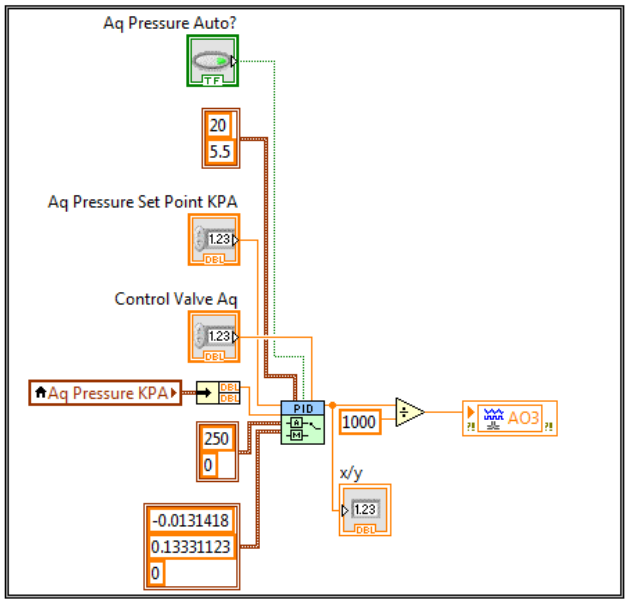

b)

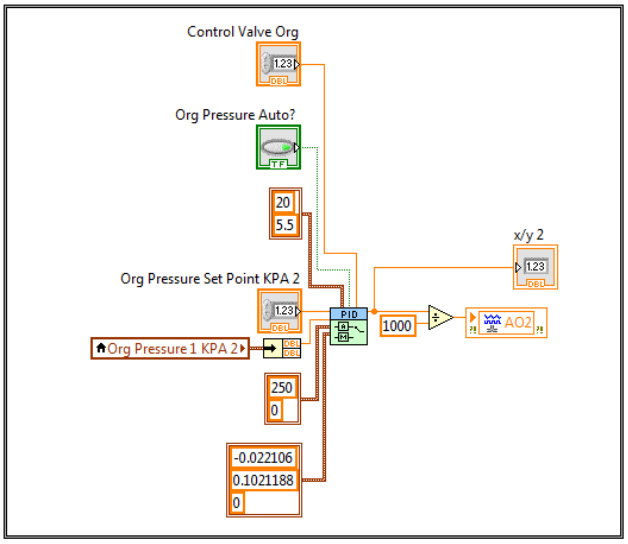

Figure 4-13: Block diagram code of the PID control used for the a) aqueous pressure and b) organic pressure.

The optimisation of the pressure control algorithms was done in a similar method to the flow rate optimisation. The optimisation of the aqueous pressure is presented in Figure 4-14. Similar to the flow control, P only control resulted in unstable oscillations and is thus not displayed. Although both PI and PID overshot the set point, the PI control stabilised more quickly as the rise time was slower, resulting in less over shoot. After fine tuning, it was shown that the pressure required approximately 55 seconds to reach the set point, leaving enough time for the flow rate to stabilise. The optimal PI control values were K_c = -0.0131 and T_i = 0.1333 min.

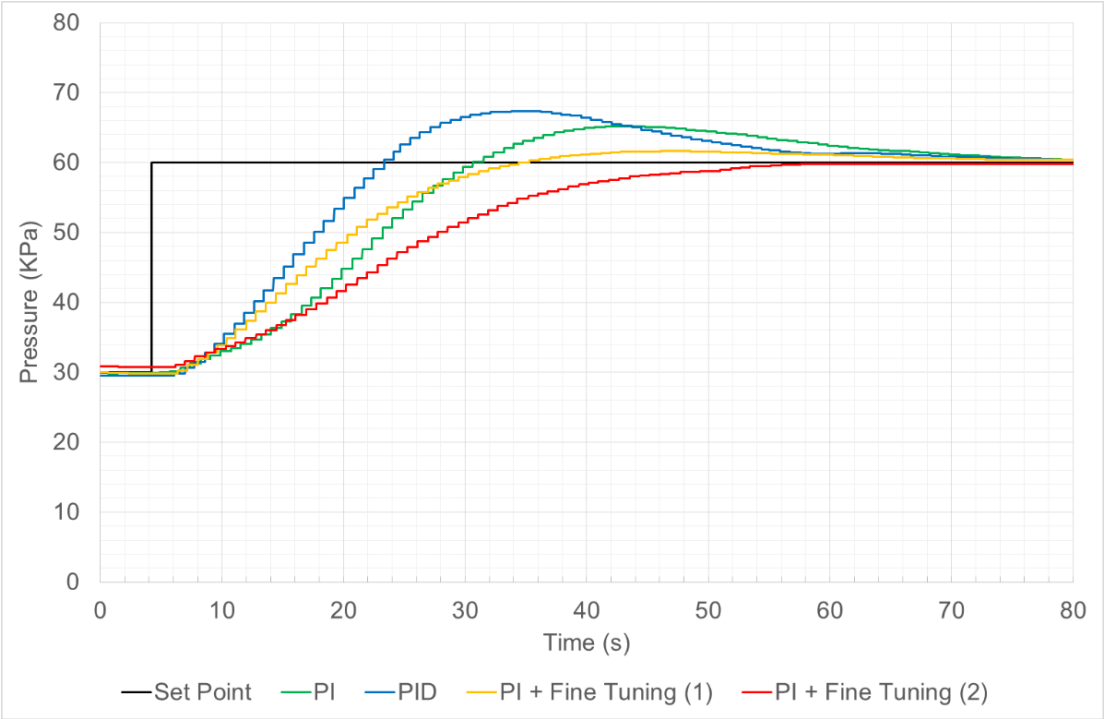

Figure 4-14: Aqueous pressure PID optimisation using Cohen-Coon and fine tuning methods

In Figure 4-15, the PID optimisation graph of the organic pressure is displayed. Both PI and PID resulted in unstable oscillations in pressure. The PI values were fine tuned to correct the formation of control oscillations. As can be seen the PI + Fine tuning (1) reduced the formation of oscillations and with further adjustment of the PI values, the optimal control values for PI were obtained as shown in PI + Fine Tuning (2). Accordingly, the pressure reached the set point after 40 seconds with the optimal control values of K_c = -0.0221 and T_i = 0.1021 min.

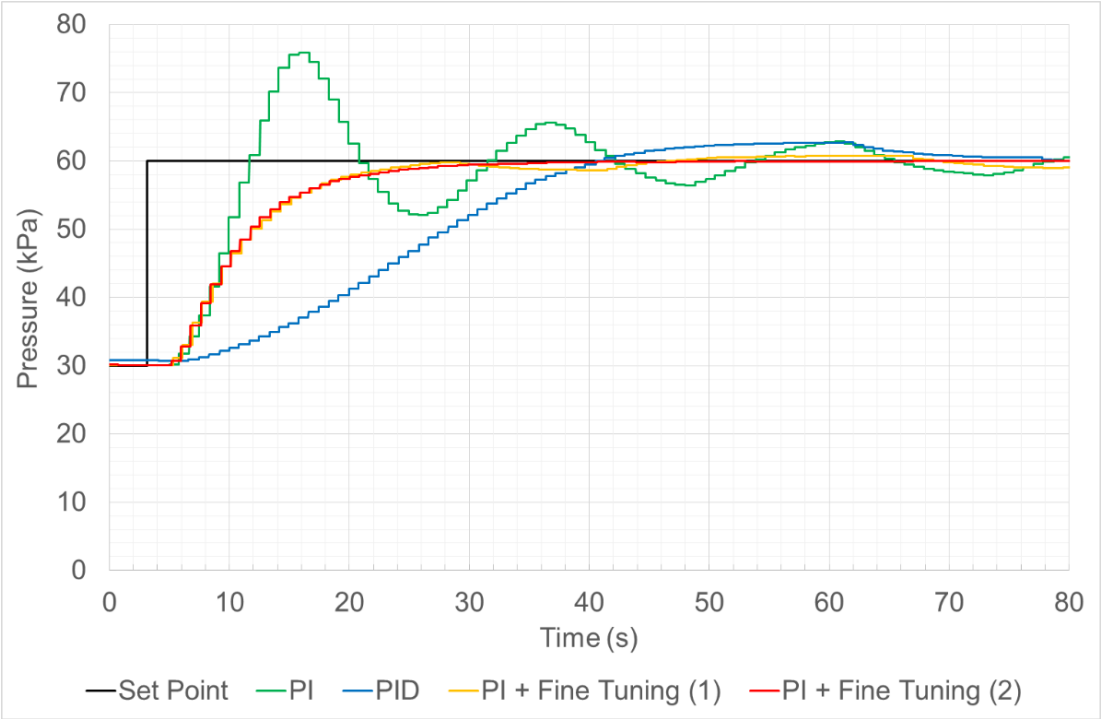

Figure 4-15: Organic pressure PID optimisation using Cohen-Coon and fine tuning methods

4.3.4 Automated sampling

The automated sampling program (and front panel) as seen in Figure 4-16, allows the user to enter the sampling times before an experiment, which when executed will deposit a 10 ml aqueous sample into a sample holder at the given time intervals. Simultaneously, 10 ml of the organic phase is removed from the organic stream and deposited into a waste container to ensure constant volume ratios throughout the experiment. The current flow rate was used to calculate the amount of time the valve had to remain open to ensure that 10 ml was being deposited into the sample holder. While the valve's opening resulted in a pressure drop, the pressure PID control was able to stabilise the pressure back to the set point as shown in Section 4.3.6.

a)

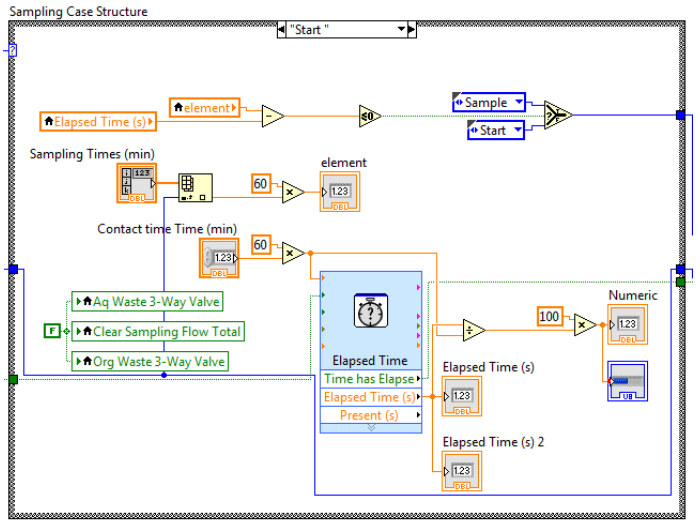

b)

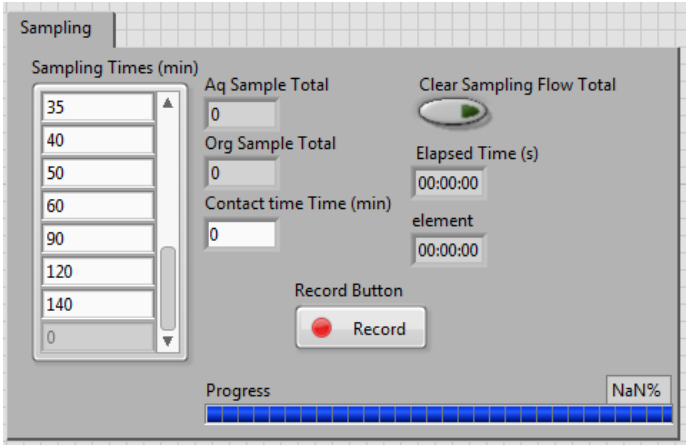

Figure 4-16: Automated sampling program a) block diagram, b) front panel

4.3.5 Internal volume and breakthrough pressure

The AMBSX total internal volume was approximately 330 ml for the aqueous side and approximately 220 ml for the organic side. Accordingly, the recommended minimum volume required for any experiment, excluding sampling (which can be calculated from the number of samples), was 350 ml for the aqueous and 250 ml for the organic feed. These small volumes required for the AMBSX imply less chemicals used, thereby reducing the cost of the experimental work.

The breakthrough was determined for the hydrophobic polypropylene membrane using cyclohexane and water. Breakthrough of the aqueous phase into the organic phase occurred with a pressure differential between 95 and 100 kPa, which correlates well with previously reported breakthrough pressures [29].

4.3.6 Case study

As mentioned previously, the extraction of Zr and Hf was evaluated using the novel AMBSX as a proof of technology investigation. For the case study, the selective extraction of Zr and Hf using Cyanex 301, as optimised by De Beer et al. [25] using batch SX (shown in Figure 4-17), was investigated using the AMBSX to evaluate the stability of the flow rate, pressure, temperature as well as the repeatability of the extraction .

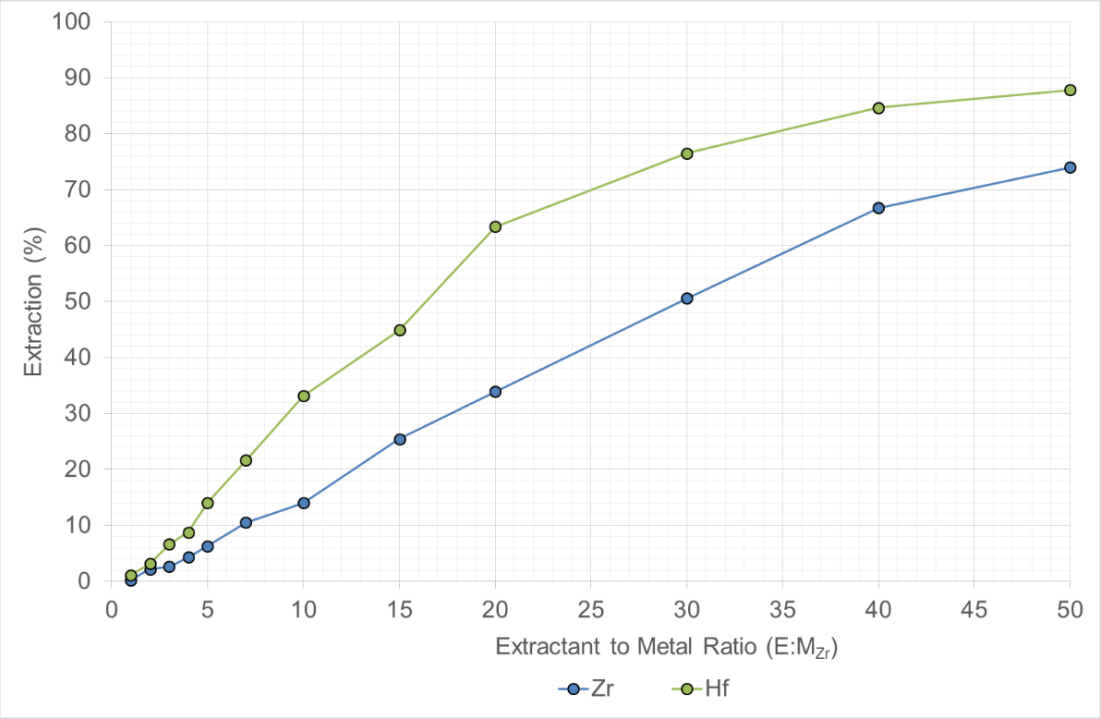

Figure 4-17: Batch solvent extraction optimisation of Zr and Hf extraction system using Cyanex 301® [25]

The individual aqueous and organic flow rates for the Cyanex 301® extraction (Repeat 1) is displayed in Figure 4-18. The flow rate over two hours is displayed with the aqueous flow rate set at 450 ml/min and the organic flow rate set at 350 ml/min. In the first minute from the system start-up, the flow rates rose abruptly, which was caused by the AMBSX system pipes being empty. At this stage the positive displacement pumps drove only air through the system, which when passing through the in-line turbine flow meter caused the turbine to spin much faster giving a higher reading than the flow rate obtained when pumping a liquid. However, once the system had filled with the solution, the flow rate stabilised. The flow rate differential of the aqueous and organic streams is important for the mass transfer during extraction. The differential flow rates of the five repeats is presented in Figure 4-19. The flow rate differential over five repeats indicates that the control of the flow rate was held constant over the two hour contact time, with little deviation from the set flow rates.

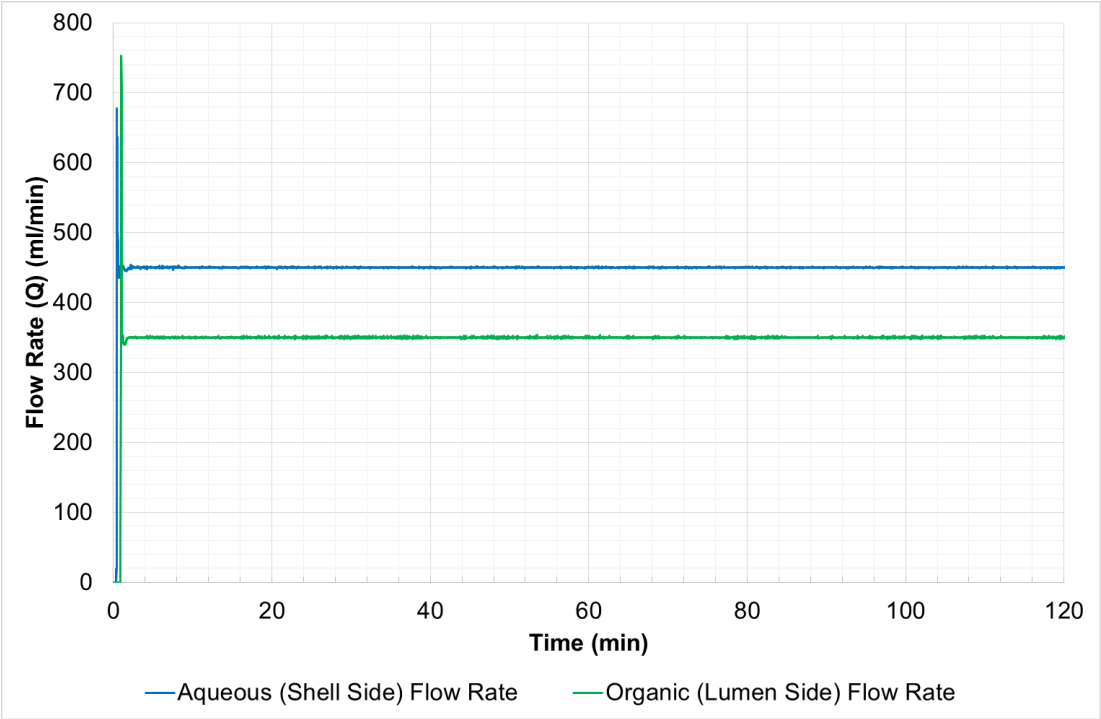

Figure 4-18: Induvial aqueous and organic (shell and lumen) flow rate of the Cyanex 301 Repeat 1

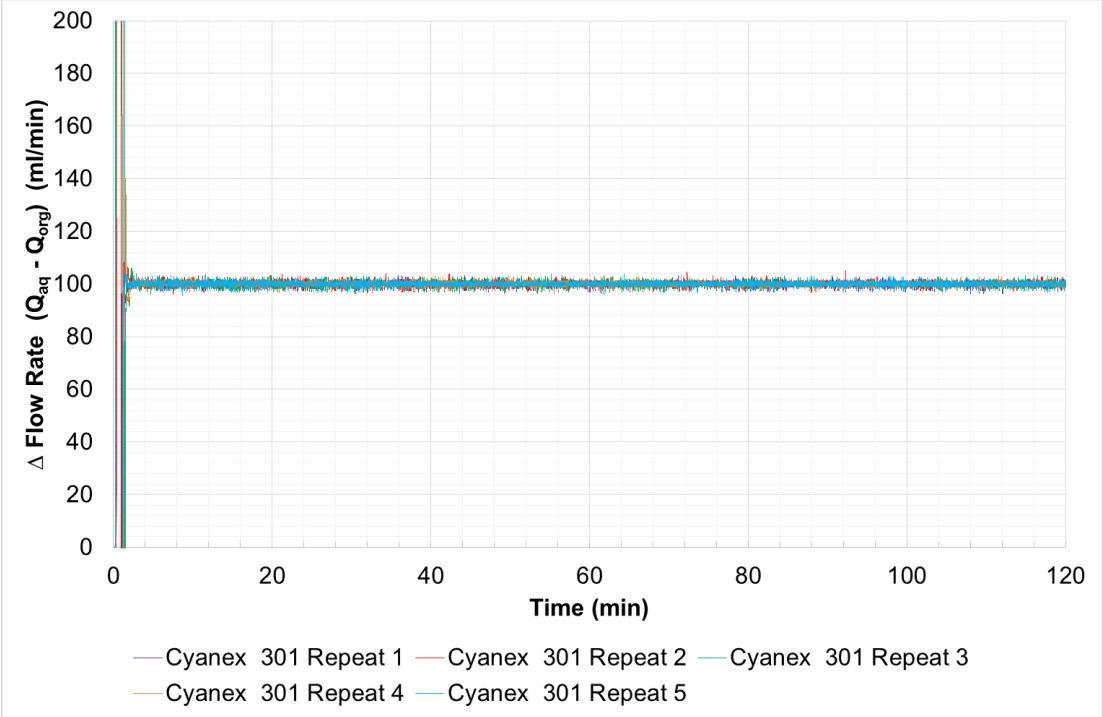

Figure 4-19: Differential flow rate (Q_{aq} – Q_{org}) of the extraction of Zr and Hf using Cyanex 301® on the AMBSX system

Figure 4-20 displays the shell side pressure differential between shell inlet and shell outlet pressure for the five repeats where the inlet pressure was controlled at 100 kPa. As in the case of the flow rate differential, the initial values were erratic due to the system start-up procedure and

filling of the system with solution. However, once the system was completely filled, the control elements were able to stabilise. It can be seen that the pressure of the system remained constant throughout the experiment with an average differential pressure of 13 kPa over the two hours.

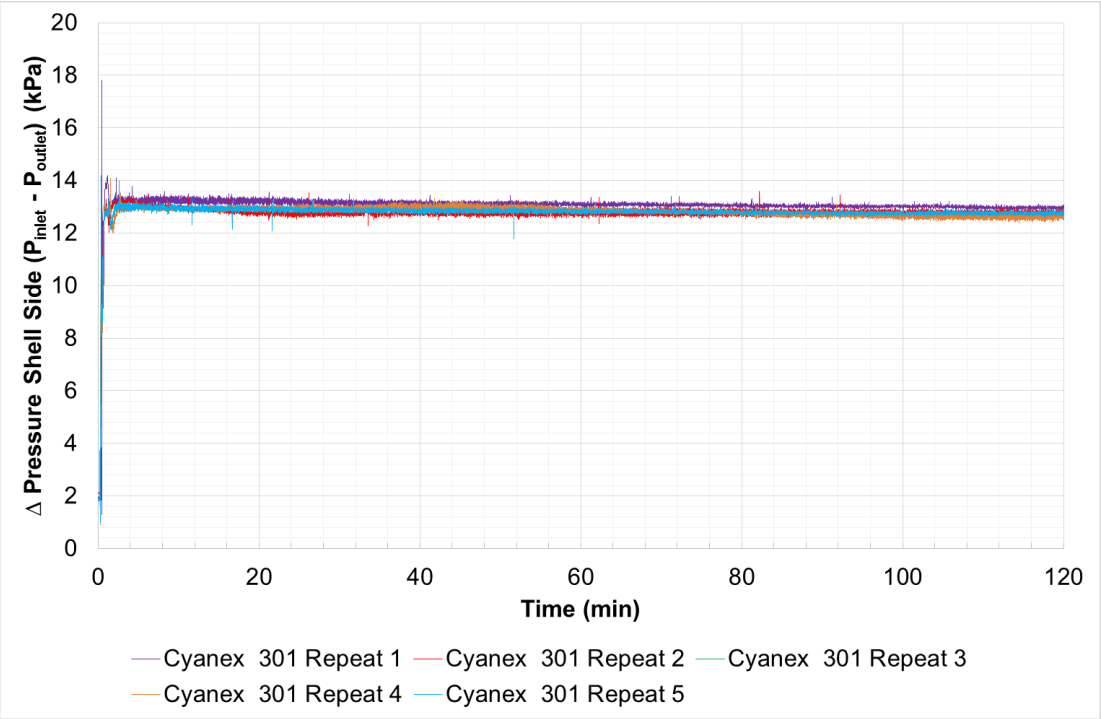

Figure 4-20: Shell side pressure differential (P_{inlet} – P_{outlet}) containing the $Zr(Hf)Cl_4$ in a 0.5M H_2SO_4 aqueous phase

In Figure 4-21, the pressure differential of the lumen side is shown. The average differential pressure was higher than on the shell side, with pressures ranging from 62 kPa to 68 kPa. This higher pressure differential is caused by a higher pressure drop over the lumen side of the membrane, as the liquid must enter the hollow fibres of the membrane. Additionally, the four three-way valves (V3-O3, V3-O4, V3-O5 and V3-O6) situated at the lumen ports compound the pressure drop over the lumen side of the membrane. This, however, does not pose a problem to the AMBSX, as long as the pressure differential over the membrane remains under 100 kPa to prevent breakthrough. Again the consistency both over time and repeating experiments is clearly demonstrated.

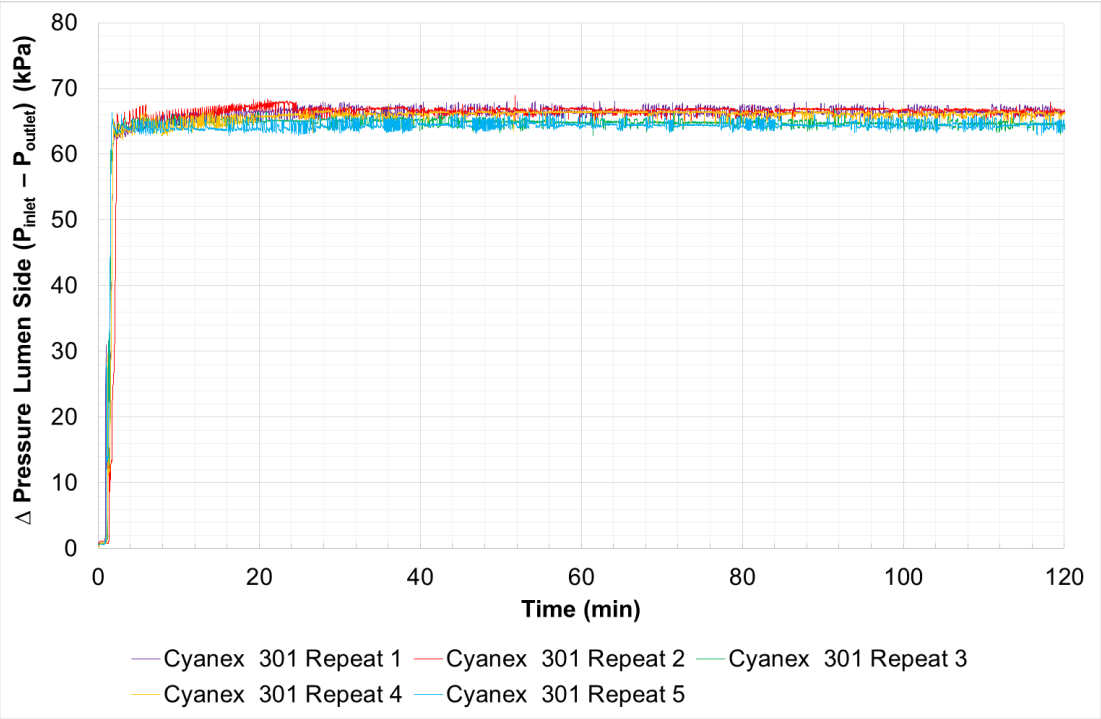

Figure 4-21: Differential pressure (P_{inlet} – P_{outlet}) for the lumen side containing the Cyanex 301® extractant dissolved in a cyclohexane and 1-octanol organic phase

While the AMBSX system was not temperature controlled, the temperatures of both the aqueous and organic feed solutions were monitored during the experiments. As an example, the temperature profile for a single run is shown in Figure 4-22. The temperatures in both feeds were approximately 25°C. Within the first 5 minutes, a 3°C drop in temperature was observed for both streams. The slight drop could have been caused by the piping and equipment's internal temperature being lower than that of the solution, cooling the solution. Over the course of the experiment (120 min), the feed solutions' temperatures slowly rose back to the starting temperatures. The temperature profile that was observed was similar in every repeat of the experiment. The temperature remains within the operating temperature limit of the hollow fibre membrane (35°C) as listed by the manufacturer [30].

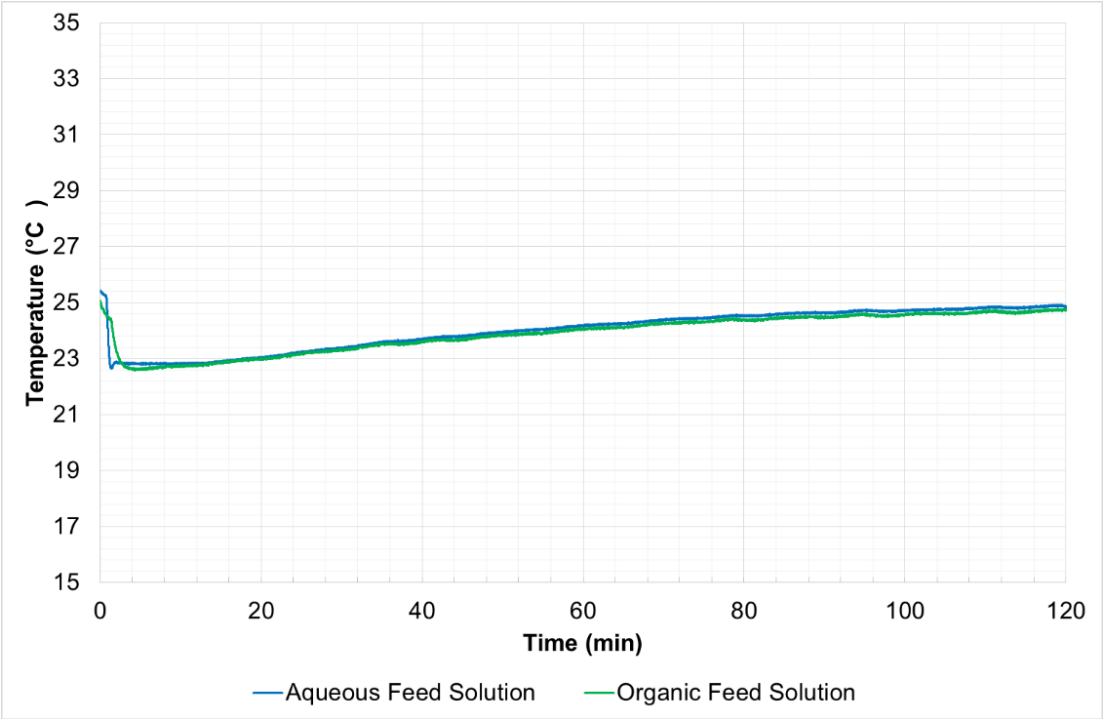

Figure 4-22: Aqueous and organic feed solutions temperature profile

After ICP-OES analysis, the metal concentrations of Zr and Hf in the aqueous samples were obtained as displayed in Figure 4-23. An average Zr starting concentration of 364 mg/L and 13.0 mg/L of Hf was found. After two hours of contact time the metal concentrations had dropped to 156 mg/L Zr and 1.3 mg/L Hf. This calculates to an average percentage extraction for the 5 repeats of 57% Zr and 90% Hf, which is an improvement of the batch SX of 50% Zr and 76% Hf, as presented in Figure 4-17. The improvement of extraction is largely due to the increase in contact area of the hollow fibre membrane, compared to the contact area of batch SX. The average standard deviation of the results was 0.6 % for Zr and 1.2% for Hf. This shows that the AMBSX not only yielded a constant flow and pressure, but that the extraction results were also highly repeatable.

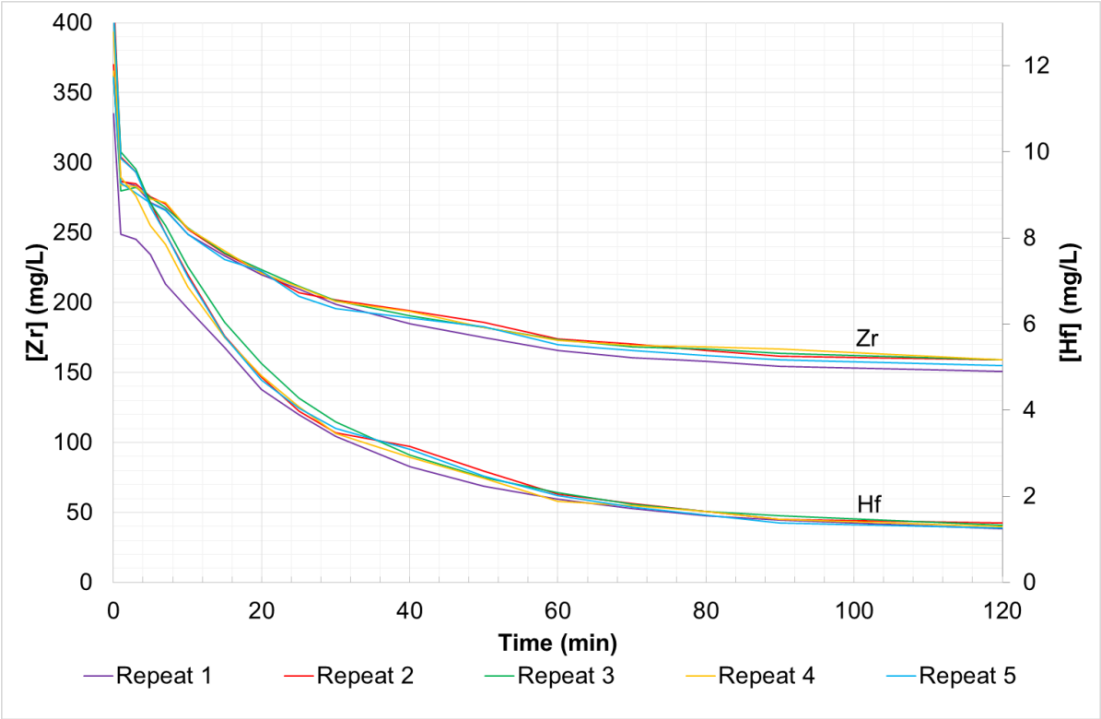

Figure 4-23: Zr and Hf metal concentration in the aqueous solution determined by ICP-OES

4.4. Conclusion

In this study, the aim of designing and building an AMBSX experimental setup was successfully implemented. The automated process was designed for a wide range of conditions commonly found in metal ion extraction. The materials used in the AMBSX were selected to withstand acids up to a concentration of 9 mol/L as well as strong organic solvents commonly used in SX research. The AMBSX system was automated using NI LabVIEW™. Using PID control it was possible to independently control both the flow rate and pressure of the aqueous and organic phases of the AMBSX. The system was able to accurately control both the aqueous and organic flow rates between 100 ml/min and 850 ml/min. The pressure was limited to a maximum pressure of 200 kPa. The flow rate, pressure and temperature of the system were recorded, which had not been possible with the previous generation of MBSX systems. Additionally, automated flow rate calibration and sampling procedures were programmed, further reducing human input in the system, while increasing the accuracy of the results.

A case study for the separation of Zr and Hf was conducted to determine both the performance and the repeatability of the AMBSX system during an extraction experiment. The AMBSX was able to control the flow rate and pressure with little to no deviation of the set point, confirming that the AMBSX remains stable during experiments, which lead to the observed repeatability of the results. As with the batch process, the AMBSX resulted in an Hf selective extraction, with an average extraction of 90% Hf and 57% Zr. The AMBSX separation results showed an

improvement from the batch SX results, with the extraction of Hf increasing with 14% from 76% and Zr increasing by 7% from 50%. The extraction experiments were repeated five times with a standard deviation of less than 1.2% between runs. It is clear that the AMBSX is suitable for further research, showing that variation in results are caused by the chemistry of the extraction and not the design of the AMBSX.

4.5. References

1. Ritcey, G., *Solvent Extraction in Hydrometallurgy: Present and Future.* Tsinghua Science & Technology, 2006. **11**(2): p. 137-152.

2. Agarwal, S., M.T.A. Reis, M.R.C. Ismael, and J.M.R. Carvalho, *Zinc extraction with Ionquest 801 using pseudo-emulsion based hollow fibre strip dispersion technique.* Separation and Purification Technology, 2014. **127**: p. 149-156.

3. Juang, R.-S. and H.-L. Huang, *Mechanistic analysis of solvent extraction of heavy metals in membrane contactors.* Journal of Membrane Science, 2003. **213**(1–2): p. 125-135.

4. Rout, P.C. and K. Sarangi, *A comparative study on extraction of Mo(VI) using both solvent extraction and hollow fiber membrane technique.* Hydrometallurgy, 2013. **133**(0): p. 149-155.

5. Fontàs, C., V. Salvadó, and M. Hidalgo, *Separation and Concentration of Pd, Pt, and Rh from Automotive Catalytic Converters by Combining Two Hollow-Fiber Liquid Membrane Systems.* Industrial & Engineering Chemistry Research, 2002. **41**(6): p. 1616-1620.

6. Gabelman, A. and S. Hwang, *Hollow fiber membrane contactors.* Journal of Membrane Science, 1999. **159**(1–2): p. 61-106.

7. San Román, M.F., E. Bringas, R. Ibañez, and I. Ortiz, *Liquid membrane technology: Fundamentals and review of its applications.* Journal of Chemical Technology and Biotechnology, 2010. **85**(1): p. 2-10.

8. Johnson, B.N. and N. Sobel, *Methods for building an olfactometer with known concentration outcomes.* Journal of Neuroscience Methods, 2007. **160**(2): p. 231-245.

9. Elliott, C., V. Vijayakumar, W. Zink, and R. Hansen, *National Instruments LabVIEW: A Programming Environment for Laboratory Automation and Measurement.* Journal of the Association for Laboratory Automation, 2007. **12**(1): p. 17-24.

10. Klocke, F., O. Dambon, U. Schneider, R. Zunke, and D. Waechter, *Computer-based monitoring of the polishing processes using LabView.* Journal of Materials Processing Technology, 2009. **209**(20): p. 6039-6047.

11. Curcio, S., V. Calabrò, and G. Iorio, *Monitoring and control of TMP and feed flow rate pulsatile operations during ultrafiltration in a membrane module.* Desalination, 2002. **145**(1–3): p. 217-222.

12. Shen, S.F., K.H. Smith, S. Cook, S.E. Kentish, J.M. Perera, T. Bowser, and G.W. Stevens, *Phenol recovery with tributyl phosphate in a hollow fiber membrane contactor: Experimental and model analysis.* Separation and Purification Technology, 2009. **69**(1): p. 48-56.

13. Trivunac, K., S. Stevanovic, and M. Mitrovic, *Pertraction of phenol in hollow-fiber membrane contactors.* Desalination, 2004. **162**(0): p. 93 - 101.

14. Kertész, R. and Š. Schlosser, *Design and simulation of two phase hollow fiber contactors for simultaneous membrane based solvent extraction and stripping of organic acids and bases.* Separation and Purification Technology, 2005. **41**(3): p. 275-287.

15. Kertész, R., M. Šimo, and Š. Schlosser, *Membrane-based solvent extraction and stripping of phenylalanine in HF contactors.* Journal of Membrane Science, 2005. **257**(1–2): p. 37-47.

16. Wannachod, T., P. Phuphaibul, V. Mohdee, U. Pancharoen, and S. Phatanasri, *Optimization of synergistic extraction of neodymium ions from monazite leach solution treatment via HFSLM using response surface methodology.* Minerals Engineering, 2015. **77**(0): p. 1-9.

17. Williams, N.S., M.B. Ray, and H.G. Gomaa, *Removal of ibuprofen and 4-isobutylacetophenone by non-dispersive solvent extraction using a hollow fibre membrane contactor.* Separation and Purification Technology, 2012. **88**(0): p. 61-69.

18. Clement, R.E. and C. Hao, *2.03 - Liquid–Liquid Extraction: Basic Principles and Automation*, in *Comprehensive Sampling and Sample Preparation*, J. Pawliszyn, Editor. 2012, Academic Press: Oxford. p. 51-63.

19. Fauci, J.L., *PLC or DCS: selection and trends.* ISA Transactions, 1997. **36**(1): p. 21-28.

20. Wu, B., V. Yufit, J. Campbell, G.J. Offer, R.F. Martinez-Botas, and N.P. Brandon. *Simulated and experimental validation of a fuel cell-supercapacitor passive hybrid system for electric vehicles*. in *Hybrid and Electric Vehicles Conference 2013 (HEVC 2013), IET*. 2013.

21. Wang, W., J. Li, and Q. Wu, *The Design of a Chemical Virtual Instrument Based on LabVIEW for Determining Temperatures and Pressures.* Journal of Automated Methods and Management in Chemistry, 2007. **2007**: p. 7.

22. Wang, L., Y. Tan, X. Cui, and H. Cui, *The Application of LabVIEW in Data Acquisition System of Solar Absorption Refrigerator.* Energy Procedia, 2012. **16, Part C**(0): p. 1496-1502.

23. Mingle, Z., Y. Jintian, J. Guoguang, and L. Gang, *System on Temperature Control of Hollow Fiber SpinningMachine Based on LabVIEW.* Procedia Engineering, 2012. **29**(0): p. 558-562.

24. Jankovec, M., *Graphical Programming Techniques for Effective, Fast and Responsive Execut*, in *Practical Applications and Solutions Using LabVIEW™ Software*, S. Folea, Editor. 2011, InTech.

25. De Beer, L., D. van der Westhuizen, and H.M. Krieg, *The selective extraction of Hf from Zr(Hf)Cl$_4$(aq) using organophosphorous derivatives*. 2016, North-West University

26. van der Westhuizen, D.J., *Separation of Zirconium and Hafnium via Solvent Extraction*, in *Chemistry*. 2010, North-West University Potchefstroom. p. 141.

27. Branken, D.J., *Separation of Zr and Hf via fractional crystallization of K2Zr(Hf)F6 : a theoretical and experimental study / D.J. Branken*. 2009.

28. Svrcek, W.Y., D.P. Mahoney, and B.R. Young, *A real-time approach to process control*. 2006: Wiley.

29. Pabby, A.K. and A.M. Sastre, *State-of-the-art review on hollow fibre contactor technology and membrane-based extraction processes.* Journal of Membrane Science, 2013. **430**: p. 263-303.

30. *2.5 X 8 EXTRAFLOW, CLAMPED* [Mechanical Drawing] 2006 26/04/2012 [cited 2015 08/10/2015]; Available from: http://www.liquicel.com/uploads/documents/2.5%20x%208%20Clamped%20with%20NPT%20ports%2012-2837%20rev4.pdf.

CHAPTER 5: EVALUATION AND RECOMMENDATIONS

5.1. Evaluation

The aim of this study was to design and construct a fully AMBSX system that can independently control flow rate and pressure, while being suitable for a wide range of experimental configurations and variables. The system must be able to conduct experiments over a range of pressures (0-200 kPa), flow rates (100-1000 ml/min) and flow directions (co- and counter-current) up to a temperature of 35°C. In addition, the system should require less human input, while simultaneously increasing the control, stability and repeatability of MBSX experiments. Finally, it should be able to record both the parameters of the system as well as the data obtained during operation.

To attain this, the project was initiated with a literature study (Chapter 2) focussing on the use of hollow fibre membranes in metal ion extraction. According to the literature, all metal ion extraction studies employing MBSX used near identical experimental setups with no or little improvements to the setups used, rather focussing on those experimental variables that determine extraction such as solvents, acids and, most notably, extractants. With the demonstration of the suitability of the technology per se, papers have been published more recently emphasizing the next stage for this technology, i.e. the use of more complex multi-staged or cascade systems [1,2]. However, the currently used manual system design will be insufficient for use in multi membrane experimental setups. This further emphasizes the necessity for research focussing on the further development and automation of the actual setup itself.

The AMBSX PFD was based on the improvement and further development of the basic design of the previous generation of MBSX setups. After the design of the PFD of the AMBSX system had been completed, the control elements of the AMBSX were simulated as a proof of concept of the control of flow rate and pressure using LabVIEW™ and PID algorithms. The direct relation and interdependence of flow rate and pressure in a closed system required proof that the flow rate and pressure could be controlled independently. This was presented in Chapter 3, in which the PID control of flow rate and pressure was simulated using LabVIEW™'s built-in simulation and PID subprograms. The simulation not only confirmed that the control of flow rate and pressure for both aqueous and organic streams was possible, it also provided information that was invaluable for the control of real AMBSX systems. Firstly, it was shown that the PI control algorithm was ideally suited for the control of flow rate and pressure in a closed loop liquid system, which confirmed observations made by Svrcek et al. [3]. Secondly, the simulation suggested that the control gain (K_c) of the aqueous and organic pressure control (electronic pressure control valve) should be negative to ensure the correct control of the electronic pressure control valves. Lastly, the flow rate control PID should have a quick response time, while the pressure control PID should

have a slower response time to prevent a resonating oscillation effect which would result in unstable flow and pressure control.

After the control simulation, the AMBSX system components were sourced and the AMBSX constructed as discussed in detail in Chapter 4. The selection of the materials used in the AMBSX system were based on their resistance to acids of up to 9 mol/L and to the strong organic solvents commonly used in extraction studies, as well as the supplier provided service life of the equipment and fittings. After construction, the simulated PID control values obtained in Chapter 3 were used as starting point to optimise the real AMBSX system. It was noted that the PID values from the simulated results differed from the AMBSX optimised PID values, which can be ascribed to the differences in the parameters (such as dead time, gain and lag time) of the simulated and the actual control elements.

After the control optimisation of the flow and pressure and its initial characterisation, it was found that the breakthrough pressure obtained (ranging from 95 kPa to 100 kPa) correlated with the reported values presented in other studies. From the volume determination it was found that the system had relatively low internal volumes for the aqueous and organic sides of 350 ml and 250 ml, respectively, which will reduce the cost of experimentation when using the AMBSX setup. While the maximum stable flow rates of 850 ml/min for both aqueous and organic sides were slightly less than the theoretically envisaged maximum flow rate of 1000 ml/min, the AMBSX was able to control the pressure up to 200 kPa, as had been aimed. While the calibration procedure of the flow meters was successful in calibrating both aqueous and organic flow rates, it was shown that solutions would have to be calibrated if different feed solutions were to be used, as the viscosity of the solution affects the accuracy of the flow rate measured by the turbine flow meters.

The case study conducted on the SX based separation of Zr and Hf confirmed that the AMBSX was successful in its original aim of a bench scale flow rate and pressure controlled MBSX setup. The control of flow rate and pressure over five repeats of the extraction experiment showed little to no deviation from the set point values for the two hour contact time experiments. While the flow rate according to the start-up procedure initially shot past the set point, this was caused by the air within the system spinning the turbine flow meter as the system fills with liquid and correct flow rates were obtained within the first minute, which did not cause any major problems to the stability of the system. Repeatability of the AMBSX was also investigated in terms of the actual extraction of Zr and Hf using a Cyanex 301® extractant. An average standard deviation of 1.2% in extraction was obtained over five repeats. This leads to the conclusion that the designed AMBSX system is able to independently control the most important experimental parameters, thereby providing repeatable extraction results, showing the suitability of this setup for further metal ion extraction studies to be conducted within the Membrane Technology group.

5.2. Recommendations

Although the automation of the MBSX experimental setup was successful in its aims of independent control of flow and pressure with a process design flexible enough to handle a wide variety of experimental conditions including chemical concentrations, flow directions, flow rates and pressures, the AMBSX system could be further improved by considering the following suggestions.

The use of multiple membrane contactors in simultaneous extraction and stripping experimental setups (as described in Chapter 2) or in a cascade setup would be the next step in upscaling and industrialising this technology. This could, however, be added to the above described process by including the components such as pump, flow meter, pressure gauges, pressure control valve, three-way valves and membrane into the PFD, as proposed in Figure 5-1 (for a combined extraction and stripping setup). No additional control hardware is needed as there are sufficient terminals open on the central controller.

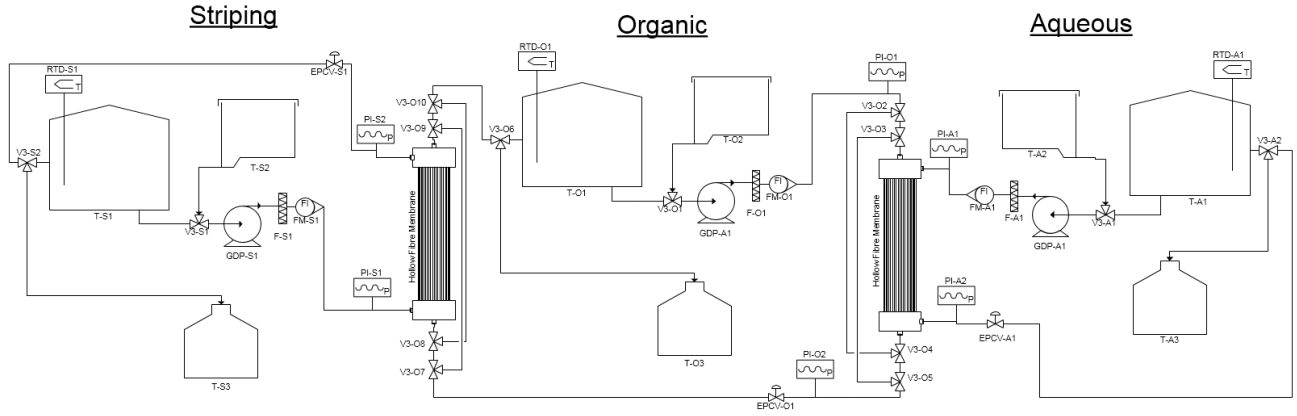

Figure 5-1: Suggested simultaneous extraction and stripping AMBSX PFD

As mentioned above, the flow meters currently have to be calibrated for different solutions to ensure accuracy of flow rates. This can be avoided by creating a data base for the commonly used solutions and corresponding K-factor values for the extraction studies. This data base could then be added into the LabVIEW™ control program, ensuring that the correct K-factor would be used according to the solution used as specified by the operator.

The AMBSX system was constructed on a temporary test bench which was adequate for the purpose of this study (see Figure 5-2). However, for the envisaged use for various applications at different locations, the system should be rebuilt in a dedicated stand that will house all the electronics and equipment in a safer, more mobile and aesthetically pleasing manner.

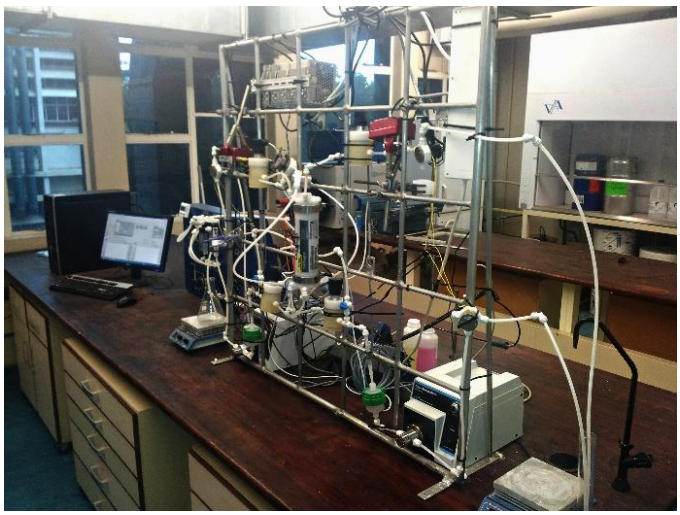

Figure 5-2: Temporary test bench setup of the AMBSX system

This envisaged case should separate the electronics from the wetted parts to protect the electronics in case of a leakage or spill of chemicals. Plans for a custom stand could for example look something like the stand displayed in Figure 5-3. The stand would house the piping in the front glass enclosed section, while the electronics, including the control computer backup power and central controller, would be in the rear section of the case. The chemical waste containers (T-A3 and T-O3) would be housed in the lower front section of the stand, with the feed solution tanks (T-A1 and T-O1) and cleaning solution tanks (T-A2 and T-O2) placed on the shelves located on the sides of the stand. The case could be temperature controlled to ensure that all equipment and piping are held at a constant temperature, which would help reduce the temperature drop shown in Figure 4-22.

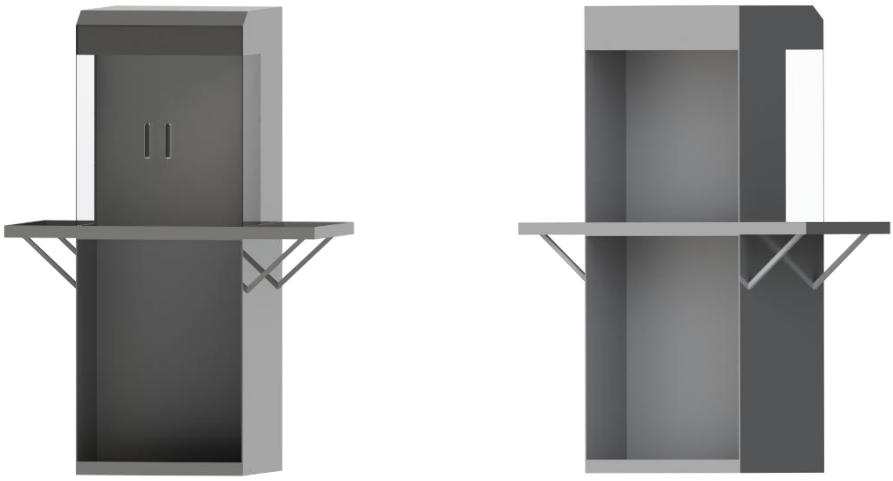

a) b)

Figure 5-3: Proposed design for custom stand for the AMBSX system showing a) the front view and b) the back view (designed and drawn using Solidworks® 2014)

While the sampling system of the AMBSX system was programmed to automatically sample the aqueous solution at the predetermined intervals, the system still required the operator to manually change the sample holders after every sampling time. This can be solved by introducing an automated sample delivery system that will work in a similar method to commercially available auto samplers. The CompaqRio controller has sufficient space and capability for an auto sampler system to be added and programmed using LabVIEW™, to either move the sampling holders past the sampling point (conveyer belt system) or to move the sampling point to sample containers (robotic arm). However, sample contamination caused by the auto sampler must be avoided to ensure that cross contamination does not take place [4].

5.3. References

1. Boributh, S., W. Rongwong, S. Assabumrungrat, N. Laosiripojana, and R. Jiraratananon, *Mathematical modeling and cascade design of hollow fiber membrane contactor for CO2 absorption by monoethanolamine.* Journal of Membrane Science, 2012. **401–402**(0): p. 175-189.

2. Gunderson, S.S., W.S. Brower, J.L. O'Dell, and E.N. Lightfoot, *Design of Membrane Cascades.* Separation Science and Technology, 2007. **42**(10): p. 2121-2142.

3. Svrcek, W.Y., D.P. Mahoney, and B.R. Young, *A real-time approach to process control*. 2006: Wiley.

4. Hurst, W.J., *Automation in the Laboratory*. 1995: VCH.